HHS Public Access

Author manuscript

Eur J Immunol. Author manuscript; available in PMC 2017 February 01.

Published in final edited form as:

Eur J Immunol. 2016 February ; 46(2): 464–479. doi:10.1002/eji.201545817.

TISSUE FACTOR EXPRESSION BY MYELOID CELLS CONTRIBUTES TO PROTECTIVE IMMUNE RESPONSE AGAINST *Mycobacterium tuberculosis* INFECTION

Sambasivan Venkatasubramanian[1], **Deepak Tripathi**[1], **Torry Tucker**[2], **Padmaja Paidipally**[1], **Satyanarayana Cheekatla**[1], **Elwyn Welch**[1], **Anjana Raghunath**[1], **Ann Jeffers**[2], **Amy R. Tvinnereim**[1], **Melissa E Schechter**[4], **Bruno B Andrade**[5,6], **Nizel Mackman**[3], **Steven Idell**[2], and **Ramakrishna Vankayalapati**[1]

[1]Department of Pulmonary Immunology, University of Texas Health Science Center at Tyler, Tyler, TX 75708, USA

[2]Department of Cellular and Molecular Biology, University of Texas Health Science Center at Tyler, Tyler, TX 75708, USA

[3]Department of Medicine, The University of North Carolina at Chapel Hill School of Medicine, NC 27516, USA

[4]Clinical Research Directorate/Clinical Monitoring Research Program, Leidos Biomedical Research, Inc., Frederick National Laboratory for Cancer Research, Frederick, MD 21702, USA

[5]Investigative Medicine Branch, Laboratory of Immune Regulation, Centro de Pesquisas Gonçalo Moniz (CPqGM), Fundação Oswaldo Cruz (FIOCRUZ), Salvador, Bahia, 40296-710, Brazil

[6]Research Center, Brazilian Institute for Tuberculosis Research, Salvador, Bahia, 45204-040, Brazil

Abstract

Tissue Factor (TF) is a transmembrane glycoprotein that plays an essential role in hemostasis by activating coagulation. TF is also expressed by monocytes/macrophages as part of the innate immune response to infections. In the current study, we determined the role of TF expressed by myeloid cells during *Mycobacterium tuberculosis* (*M. tb*) infection by using mice lacking the TF gene in myeloid cells (TF^{Δ}) and human monocyte derived macrophages (MDMs). We found that during *M. tb* infection, a deficiency of TF in myeloid cells was associated with reduced inducible nitric oxide synthase (iNOS) expression, enhanced arginase 1 (Arg1) expression, enhanced IL-10 production and reduced apoptosis in infected macrophages, which augmented *M. tb* growth. Our results demonstrate that a deficiency of TF in myeloid cells promotes M2 like phenotype in *M .tb* infected macrophages. A deficiency in TF expression by myeloid cells was also associated with reduced fibrin deposition and increased matrix metalloproteases (MMP)-2 and MMP-9 mediated

Corresponding author: Ramakrishna Vankayalapati, Department of Pulmonary Immunology, University of Texas Health Center at Tyler, 11937 US Highway 271, Tyler, TX 75708-3154, telephone (903) 877-5190, fax (903) 877-7989, krishna.vankayalapati@uthct.edu.

Conflict of interest:
The authors declare no commercial or financial conflict of interest.

inflammation in *M. tb* infected lungs. Our studies demonstrate that TF expressed by myeloid cells has newly recognized abilities to polarize macrophages and to regulate *M. tb* growth.

Keywords

Tissue factor; Macrophage; IL-10; *M. tuberculosis*; Apoptosis

Introduction

Tuberculosis (TB) is a leading cause of death world-wide that, claims an estimated 1.3 million lives annually [1, 2]. *Mycobacterium tuberculosis (M. tb)* can proliferate and survive in alveolar and tissue macrophages, which favor the establishment and progression of infection, and has the capacity to persist and reactivate disease even decades later. To develop new tools to prevent tuberculosis, it is important to identify the factors that regulate inflammation and the intracellular growth of *M. tb* in macrophages.

Tissue Factor (TF) also known as factor III, tissue thromboplastin, and CD142 is a 47 kD transmembrane glycoprotein that belongs to the cytokine receptor superfamily and that plays an essential role in hemostasis by activating coagulation [3, 4]. TF is also expressed in a wide range of cancers, metabolic diseases and infections and contributes to inflammation, angiogenesis and apoptosis [3–6]. TF is constitutively expressed by various cell types, including vascular smooth muscle cells, fibroblasts, and epithelial cells, and can be induced in activated monocytes/macrophages and endothelial cells [6–9]. For instance, bacterial products such as lipopolysaccharide induce TF expression in monocytes [6–8]. This response is thought to be part of the innate immune system that reduces the dissemination of pathogens. Previous studies have shown that human monocyte derived macrophages (MDMs) express TF in response to *M. tb* exposure [10]. A recent study using low TF expressing mice in *M. tb* suggested that TF exerts a limited role in TB pathogenesis [11]. We posited that specific deletion of TF in myeloid cells could enhance pulmonary *M. tb* infection and sought to test this inference in the present study. We used mice lacking the TF gene specifically in myeloid cells ($TF^{fl/fl}$, LysMCre), which are referred to as TF^{Δ} mice and human MDMs with reduced TF expression. We found that during *M. tb* infection, a deficiency of TF in myeloid cells was associated with the polarization of macrophages to a more M2 like phenotype, enhanced IL-10 production and reduced apoptosis of infected macrophages which augmented *M. tb* growth. In addition, a deficiency of TF expression by myeloid cells was associated with reduced fibrin deposition and enhanced matrix metalloproteases (MMP)-2 and MMP-9-mediated inflammation in *M. tb* infected lungs.

Results

TF expression and bacterial burden in M. tb infected wild type C57BL/6 mice

To determine if TF expression increases with bacterial burden, C57BL/6 mice were infected with *M. tb* H37Rv by aerosol. One, two, three, four and eight weeks after infection, TF expression in the lungs were determined using real-time PCR. As shown in Fig. 1A, after one week the number of CFU was $2.4 \pm 0.2 \times 10^3$, and this increased to $1.1 \pm 0.2 \times 10^4$ CFU

($p<0.05$), $1.5 \pm 0.5 \times 10^5$ CFU ($p<0.05$), $0.9 \pm 0.2 \times 10^6$ CFU, and $0.74 \pm 0.15 \times 10^6$ CFU per lung ($p<0.05$) by the 2nd, 3rd 4th and 8th week after infection, respectively. We also measured TF expression in the lungs at weekly intervals. As shown in Fig. 1B, one week after *M. tb* infection TF expression was upregulated 2.69-fold compared to uninfected mice lungs ($p<0.05$). This was increased to 5.7-fold ($p<0.05$), 8.2-fold ($p<0.05$), 5.3-fold ($p<0.05$) and 6.8-fold ($p<0.05$) after the 2nd, 3rd 4th and 8th week of infection, respectively. Our results indicate that TB infection is associated with an increased TF expression in the lungs.

TF expression by myeloid cells controls M. tb growth

To determine the role of TF expressed by myeloid cells in the control of *M. tb* growth, we infected mice lacking the TF gene in their myeloid cells (TF^{Δ} mice) and control mice ($TF^{fl/fl}$) with *M. tb* H37Rv by aerosol as described in the methods section. Thirty days after infection, the bacterial burden in the lungs, spleen, mediastinal lymph nodes (MLN) and liver was determined. There was a marginal, but significant increase in the number of bacteria in TF^{Δ} mice lung than $TF^{fl/fl}$ mice ($1.9 \pm 0.1 \times 10^6$ vs. $3.7 \pm 0.2 \times 10^6$, $p=0.0005$, Fig. 2A). In the spleen (Fig. 2B), MLN (Fig. 2C) and liver (Fig. 2D) the number of CFU was significantly higher in TF^{Δ} mice compared to $TF^{fl/fl}$ mice. Sixty days after infection, there was a similar increase in bacterial burden in the lungs, spleen, MLN and liver (Supporting Information Fig. 1). To confirm that increased *M. tb* growth in TF^{Δ} mice is due to lack of the TF gene expression in macrophages, we isolated peritoneal exuded macrophages (PEMs) from control TF^{Δ} mice and control $TF^{fl/fl}$ mice and infected them with *M. tb*. The CFU were quantified after 2 h and after 5 d. In 3 independent experiments, at 2 h after infection CFU were similar in TF^{Δ} and $TF^{fl/fl}$ PEMs (Fig. 2E) suggesting that both TF^{Δ} and $TF^{fl/fl}$ macrophages were infected by *M. tb* H37Rv with similar efficiency. However, at 5d post-infection, CFU in TF^{Δ} mouse PEMs were $6.1 \pm 0.9 \times 10^6$ compared to $1.5 \pm 0.7 \times 10^6$ in $TF^{fl/fl}$ mice PEMs ($p=0.02$; Fig. 2E).

Immunohistochemical analysis of M. tb infected TF^{Δ} and $TF^{fl/fl}$ mice lungs

We next asked whether the lack of TF gene in myeloid cells had any effect on inflammatory and anti-inflammatory responses upon *M. tb* infection. TF^{Δ} and $TF^{fl/fl}$ mice were infected with *M. tb* H37Rv. After 30 days, lungs from TF^{Δ} and $TF^{fl/fl}$ control and *M. tb* infected mice were isolated, formalin fixed and paraffin-embedded. From these tissues, tissue sections were prepared and stained with hematoxylin and eosin. Histological analyses demonstrated more inflammation throughout the lungs of the *M. tb* infected TF^{Δ} mice than in the $TF^{fl/fl}$ mice (Fig. 3A). In addition to inflammation, as shown in Fig. 3B, there was a significant increase in foamy macrophages and small granulomas in the lung sections of *M. tb* infected TF^{Δ} mice. *M. tb* infection led to development of IL-10 producing, less phagocytic and less bactericidal foamy macrophages [12]. We next determined whether the foamy macrophages are the source of increased IL-10. The above described *M. tb* infected TF^{Δ} and $TF^{fl/fl}$ mouse lung sections were next examined for IL-10+ foamy macrophages. As shown in Fig. 3C, 62.4 ± 8.4 % of *M. tb* infected TF^{Δ} mice alveolar macrophages were IL-10+ compared with 31.2 ± 3.4 % of alveolar macrophages in the *M. tb* infected $TF^{fl/fl}$ mice ($p=0.009$; Fig. 3C). Our results demonstrate that lack of TF expression by myeloid cells is associated with increased cell infiltration and anti-inflammatory responses in lung tissue upon *M. tb* infection.

Macrophages from M. tb infected TF$^{\Delta}$ mouse produce more IL-10 and are less apoptotic and assume a M2 like phenotype

To confirm the results of the above immunohistochemical analyses and determine whether the increased *M. tb* growth seen in Fig. 2 was related to enhance IL-10 production in *M .tb* infected TF$^{\Delta}$ mice, we infected TF$^{\Delta}$ and TF$^{fl/fl}$ mice with *M. tb* H37Rv. After 30 days IL-10 levels in the lungs of these mice were measured using real-time PCR. As shown in Fig. 4A, *M. tb* infected TF$^{\Delta}$ mice had 3-fold higher levels of IL-10 mRNA (p=0.0004) in their lungs compared to *M. tb* infected TF$^{fl/fl}$ mice. We also measured iNOS and Arg1 expression by real-time PCR. As shown in Fig. 4, *M. tb* infected TF$^{\Delta}$ mice had less iNOS (p=0.05, Fig. 4B) and 3 fold more Arg1 mRNA (p=0.02, Fig. 4C) in their lungs than the *M. tb* infected TF$^{fl/fl}$ mice. There was a similar decrease in iNOS expression and increase in Arg1 expression in the lungs at 60 days after infection in *M. tb* infected TF$^{\Delta}$ mice compared to *M. tb* infected TF$^{fl/fl}$ mice (Supporting Information Fig. 2 F and G).

Previously, we found that, transcription factor c-Maf enhanced IL-10 production in *M. tb* infected macrophages [13]. We measured c-Maf expression in the above lung samples. As shown in Fig. 4D, *M. tb* infected TF$^{\Delta}$ mice expressed 2.5-fold more c-Maf mRNA (p=0.01) in their lungs compared to *M. tb* infected TF$^{fl/fl}$ mice. IL-10 enhances *M. tb* growth in macrophages by decreasing apoptosis in *M. tb* infected macrophages [14–16]. We next determined the levels of apoptotic cells in the lungs of *M. tb* infected TF$^{\Delta}$ and TF$^{fl/fl}$ mice by TUNEL assay. As shown in Fig. 4E, 7.6 ± 1.6 % of the *M. tb* infected TF$^{\Delta}$ mouse alveolar cells were apoptotic compared to 16.4 ± 2.3 % of the alveolar cells in *M. tb* infected TF$^{fl/fl}$ mice (p=0.01; Fig. 4E). In other experimental systems it has been shown that disrupting mitochondrial membrane potential (ΔΨm) leads to apoptosis [17–19]. Thirty days after *M. tb* infection we quantified ΔΨm in *M. tb* infected TF$^{\Delta}$ and TF$^{fl/fl}$ alveolar cells. As shown in Fig. 4F, 9.4 ± 3 % of *M. tb* infected TF$^{\Delta}$ mice alveolar cells show loss of ΔΨm compared to 34.5 ± 18.7 % of alveolar cells in the *M. tb* infected TF$^{fl/fl}$ mice suggesting that lack of TF expression by myeloid cells leads to reduced loss of ΔΨm.

To determine if macrophages from *M. tb* infected TF$^{\Delta}$ mouse express reduced levels of iNOS, increased levels of Arg1 and produce more IL-10, we isolated PEMs from control TF$^{\Delta}$ and TF$^{fl/fl}$ mice and infected them with *M. tb* H37Rv. After 72 h, culture supernatants were collected and IL-10 levels were measured by ELISA. As shown in Fig. 4G, *M. tb* infected TF$^{\Delta}$ mice PEMs produced 3 fold more IL-10 (733.0 ± 135.0 vs. 234.5 ± 43.0 pg/ml, p=0.02, Fig. 4G) compared to *M. tb* infected TF$^{fl/fl}$ PEMs. Real-time PCR analysis of the above cultured cells was performed to quantify levels of iNOS, Arg1 and CD163 expression. As shown in Fig. 4H, *M. tb* infected TF$^{\Delta}$ PEMs expressed ∼2-fold less iNOS (p=0.03, Fig. 4H), 2-fold more Arg1 (p=0.04, Fig. 4I) and 3-fold more CD163 (p=0.03, Fig. 4J) mRNA than *M. tb* infected TF$^{fl/fl}$ mouse PEMs.

To confirm that *M. tb* infected TF$^{\Delta}$ mouse macrophages were less apoptotic, we isolated PEMs from control TF$^{\Delta}$ and TF$^{fl/fl}$ mice, infected them with *M. tb* H37Rv and quantified the apoptotic cells after 72 h by TUNEL assay. As shown in Fig. 4K, 3.8 ± 1.2 % of *M. tb* infected TF$^{\Delta}$ mouse and 8.4 ± 1.4 % of *M. tb* infected TF$^{fl/fl}$ mouse PEMs were apoptotic (p=0.04). As shown in Fig. 4L, 7.4 ± 2.9 % of *M. tb* infected TF$^{\Delta}$ mouse PEMs and 23 ± 4.7

% of wild type PEMs show loss of ΔΨm suggesting that lack of TF expression by myeloid cells leads to reduced loss of ΔΨm (p=0.02) and less apoptosis. Collectively, our results suggest that lack of TF expression polarizes *M. tb*-infected macrophages towards an M2 like phenotype.

Increased inflammation in M. tb infected TF^{Δ} mouse lungs is not due to IFN-γ and IL-17

We have shown that there is augmented growth of *M. tb* and inflammation in the lungs of *M. tb* infected TF^{Δ} mice. We next aimed to investigate whether these processes are due to increased Th1 or Th17 cytokines producing T-cells. TF^{Δ} and $TF^{fl/fl}$ mice were infected with *M. tb* and after 30 days the number of CD4+ and CD8+ cells in the lungs of control and *M. tb* infected mice were determined. As shown in Fig. 5A, the number of CD4+ cells in the lungs of *M. tb* infected TF^{Δ} lungs was significantly higher than in *M. tb* infected $TF^{fl/fl}$ mouse lungs ($4.8 \pm 0.8 \times 10^4$ vs. $1.8 \pm 0.3 \times 10^4$; p=0.009). Similarly, there were $2.1 \pm 0.4 \times 10^4$ CD8+ cells in *M. tb* infected TF^{Δ} mouse lungs compared to $0.8 \pm 0.07 \times 10^4$ in *M. tb* infected $TF^{fl/fl}$ mouse lungs (p=0.01; Fig. 5B). Because the pro-inflammatory cytokines IFN-γ, IL-12, IL-17 and IL-1β plays important roles in the regulation of *M. tb* growth, we next determined the expression levels of IFN-γ, IL-12, IL-17 and IL-1β in control and *M. tb* infected TF^{Δ} and $TF^{fl/fl}$ mouse lungs. After 30 days of *M. tb* H37Rv infection, IFN-γ and IL-17 levels in the lung were measured by real-time PCR in TF^{Δ} and $TF^{fl/fl}$ mice. As shown in Fig. 5C, *M. tb* infected TF^{Δ} mice had 33-fold less IFN-γ (p=0.02), 11-fold less IL-12 (p=0.02; Fig. 5D), and 38-fold less IL-17 (p=0.003, Fig. 5E) mRNA in their lungs compared to *M. tb* infected $TF^{fl/fl}$ mice. However, there was no significant change in IL-1β expression (Fig. 5F). A similar change in cytokines expression was found 60 days after infection (Supporting Information Fig. 2 A to E). We also measured IFN-γ and IL-17 expression in the lungs of *M. tb* infected TF^{Δ} and $TF^{fl/fl}$ mice by immunohistochemical analysis. Thirty days after infection, as shown in Fig. 5G, the mean H score for IFN-γ was 32.3 ± 7.6 in *M. tb* infected TF^{Δ} mice lungs compared to 73.4 ± 12.9 in *M. tb* infected $TF^{fl/fl}$ mouse lungs (p=0.02; Fig. 5G). Similarly, the mean H score for IL-17 was 14.4 ± 3.7 in *M. tb* infected TF^{Δ} mouse and 35.09 ± 7.6 in *M. tb* infected $TF^{fl/fl}$ mouse lungs (p=0.04; Fig. 5H). Sixty days after infection, a similar decrease in IFN-γ and IL-17 expression in the lungs of *M. tb* infected TF^{Δ} mice was found compared to *M. tb* infected $TF^{fl/fl}$ mice (Supporting Information Fig. 3).

TF expression by myeloid cells regulates MMP-2 and MMP-9 mediated inflammation

The above results suggest that increased IFN-γ and IL-17 is not responsible for the augmented inflammation in the lungs of *M. tb* infected TF^{Δ} mice. In *M. tb* infection, MMPs also plays an important role in the induction of lung inflammation [20, 21]. To determine whether MMP's are responsible for augmented lung inflammation we observed in the TF^{Δ} mice, we measured MMP-2 and MMP-9 expression in the lungs of infected TF^{Δ} and $TF^{fl/fl}$ mice. Lungs from TF^{Δ} and $TF^{fl/fl}$ control and *M. tb* infected mice were isolated, after which tissue sections were prepared and examined for MMP-2 and MMP-9 expression. As shown in Fig. 6 A and B, there was significant increase in MMP-2 and MMP-9 expression in the lungs of *M. tb* infected TF^{Δ} mouse compared to levels in $TF^{fl/fl}$ mouse lungs. As shown in Fig. 6A, the mean H score for MMP-2 was 164.8 ± 25.9 in *M. tb* infected TF^{Δ} mouse lungs compared to 96 ± 6.1 in *M. tb* infected $TF^{fl/fl}$ mouse lungs (p=0.04; Fig. 6A). Similarly, the

mean H score for MMP-9 was 206.7 ± 23.8 in *M. tb* infected TF^{Δ} mouse lungs compared to 98 ± 9.8 in *M. tb* infected $TF^{fl/fl}$ mouse lungs (p=0.005; Fig. 6B).

TF expressed by myeloid cells increases fibrin/fibrinogen deposition in M. tb infected mice

Because TF initiates coagulation, we next assessed fibrin formation in the lung samples of TF^{Δ} and $TF^{fl/fl}$ control and *M. tb* infected mice. As shown in Fig. 6C, there was less extravascular fibrin/fibrinogen in the *M. tb* infected TF^{Δ} mice compared to the *M. tb* infected $TF^{fl/fl}$ mice. MMPs can regulate fibrin deposition and fibrin plays an important role in granuloma formation and the containment of bacterial pathogens. As shown in Fig. 6C, the mean H score for fibrin/fibrinogen in *M. tb* infected TF^{Δ} mice was 70.2 ± 14.4 compared to 145.1 ± 18.8 in *M. tb* infected $TF^{fl/fl}$ mice (p=0.01).

TF regulates M. tb growth and inflammatory responses in human MDMs

To broach the relevance of the above findings to human *M. tb* infection, we examined TF expression in CD14+ monocytes in response to *M. tb*. Human PBMC were cultured with or without γ-irradiated *M. tb* (10 μg/ml) and the expression of TF was measured by intracellular staining. As shown in Fig. 7A, γ-irradiated *M. tb* significantly induced TF expression in CD14+ monocytes compared to control monocytes (13.69 ± 1.6 %vs. 0.09 ± 0.01 %, p=0.0006). As a control, we measured TNF-α production in CD14+ monocytes (11.4 ± 0.76 % vs. 0.23 ± 0.03 %, p=0.0006, Fig. 7B). The gating strategy is shown in Supporting Information Fig. 4. We also examined the expression of TF by *M. tb* infected human MDMs. As shown in Fig. 7D and as anticipated, *M. tb* infection significantly upregulated TF expression by MDMs compared to control MDMs (4.5 ± 1.9-fold, p=0.03). To determine the role of TF in IL-10 production, we next silenced TF expression in MDM and infected with *M. tb* and after 72 h, IL-10 levels in the culture supernatants were analyzed by ELISA. TF siRNA inhibited TF expression by 70% (Fig. 7D). As shown in Fig. 7E, *M. tb* infection induced IL-10 production from 14.10 ± 1.591 pg/ml to 117.3 ± 13.94 pg/ml. TF siRNA enhanced IL-10 production by 2 fold compared to control siRNA (149.9 ± 15.69 vs. 89.59 ± 13.11 pg/ml, p=0.02, Fig. 7E). Similarly, TF siRNA enhanced c-Maf expression by *M. tb* infected MDMs (5.6 ± 1.2-fold vs 1.9 ± 0.8-fold, p=0.03, Fig. 7F). Compared to the control siRNA, the TF siRNA inhibited apoptosis (3.8 ± 1.2 % vs. 1.6 ± 0.6 %, p=0.006, Fig. 7G) and disrupted the mitochondrial membrane potential in *M. tb* infected MDMs (21.4 ± 3.7 % vs 11.1 ± 3.5%, p=0.002, Fig. 7H). We also determined the effect of TF siRNA on *M. tb* growth in MDMs. In 3 independent experiments, CFU in TF siRNA transfected MDMs were 2 fold higher than control siRNA transfected MDMs (p=0.03; Fig. 7H). In contrast to the above findings, IL-10 siRNA enhanced apoptosis in *M. tb* infected MDMs (p= 0.004, Fig. 7G) and reduced *M. tb* growth (p= 0.03, Fig. 7I).

Discussion

In the current study, we found that TF expressed by macrophages regulates *M. tb* growth and, dissemination in addition of inflammation, providing the evidence that TF contributes to effective immunity against this intracellular pathogen. Our studies also demonstrate that deficiency of TF in myeloid cells polarizes macrophages to a more towards M2 like phenotype. TF expression in *M. tb* infected wild type mice correlated with bacterial burden.

Lack of TF expression by myeloid cells enhanced the bacterial burden in the lungs and other lymphoid organs in *M. tb* infected mice and TF deficient macrophages were more susceptible to *M. tb* infection. TF mediated growth inhibition involved the inhibition of IL-10 production and the enhancement of lung macrophage apoptosis. In *M. tb* infected mice, the absence of myeloid cell-produced TF reduced fibrin deposition, enhanced MMP-2 and MMP-9 mediated inflammation in the lungs and caused dissemination of disease. TF siRNA reduced apoptosis and enhanced IL-10 production and *M. tb* growth in human MDMs.

TF is an integral membrane glycoprotein that initiates blood coagulation and provides additional protection to vital organs such as the brain, lungs and heart from mechanical injury [3, 5, 6]. Excessive TF production has been observed in several disease conditions such as cardiovascular diseases, cancers, diabetes, and obesity [3–5]. TF has also been implicated in angiogenesis, wound repair, embryonic development and innate immune responses to pathogens [6, 8, 22, 23]. TF overexpression has likewise been observed in bacterial, viral, or parasitic infection [8]. Recent studies with low TF expressing mice have revealed reduced coagulation, inflammation, and mortality in these mice upon the administration of high-dose LPS [8, 24]. A recombinant human TF pathway inhibitor exerts anticoagulant, anti-inflammatory and antimicrobial effects in a model of murine pneumococcal pneumonia [25], suggesting an important role for TF in infections. A deficiency of TF in hematopoietic cells was associated with reduced LPS-induced coagulation, inflammation, and mortality, which suggests that hematopoietic cells are the major pathologic site of TF expression during endotoxemia [24, 26]. In contrast to the above acute bacterial infections, *M. tb* infected transgenic mice expressing human TF, at either very low levels (low TF) or near to the level of wild-type mice (HTF) were able to control *M. tb* infection and dissemination with comparable efficiency [11]. However, TF in lung tissues was 100-fold lower in the low TF mice compared to the HTF mice, whereas *M. tb* infected bone marrow-derived macrophages from the low TF mice expressed ∼30% the TF activity of that was observed in *M. tb* infected bone marrow-derived macrophages from HTF mice. These results suggest TF expression was insufficiently reduction of in macrophages in this model to impact *M. tb* infection [11]. In the current study, we deleted the TF gene in myeloid cells of mice and infected them with *M. tb*. We found that TF expressed by myeloid cells regulates bacterial growth and dissemination in addition to inflammation during *M. tb* infection. We also found TF siRNA inhibits *M. tb* growth in human MDMs.

We found that lack of TF expression by myeloid cells enhances IL-10 production in response to *M. tb*, which suggests that TF may regulate IL-10 production in myeloid cells via c-Maf during *M. tb* infection. IL-10 is an anti-inflammatory cytokine that is produced mainly by myeloid cells and T-cells [27–31]. IL-10 production inhibits protective immune responses and enhances susceptibility to *M. tb* and other intracellular pathogen infections [12, 32, 33]. IL-10 also inhibits various pathways that are essential for the production of pro-inflammatory cytokines such as TNF-α and anti-microbial mechanisms of myeloid cells which are both essential to controlling *M. tb* growth [34, 35]. In addition, IL-10 inhibits TF mRNA and protein expression and reduces TF levels in circulation, but the effects of TF on IL-10 production have not previously been described [36]. In the current study, we found

that *M. tb*-infected macrophages from TF^{Δ} and TF siRNA-transfected *M. tb*-infected human MDMs expressed more c-Maf, produced more IL-10, were less apoptotic and were unable to restrict *M. tb* growth compared to control macrophages. Previously we found that the transcription factor c-Maf enhances IL-10 production to regulate the growth of *M. tb* H37Rv in subpopulations of human MDMs [13]. In the current study we found that lack of TF expression enhanced c-Maf expression and IL-10 production. c-Maf is associated with the differentiation of monocytes into macrophages [37]. In the T-cell response to infection, c-Maf is a master regulator of Th2 responses, inducing the production of IL-10, IL-4 and IL-21 by binding to a c-Maf response element in the promoter regions of their encoding genes [38–43]. Bacterial adenylate cyclase toxins increase c-Maf expression and the expansion of Th2 cells [44]. Our findings demonstrate that in the absence of TF expression, pathogens can modulate c-Maf expression in mononuclear phagocytes to enhance bacterial growth. Alveolar macrophages are the first cells to interface with *M. tb* and our study suggests that during the early stages of *M. tb* infection, inflammatory responses mediated by TF inhibit c-Maf expression and IL-10 production. These interactions effectively control *M. tb* infection. Additional studies are needed to understand the specific TF mediated signaling pathways that regulate c-Maf expression.

Activated macrophages are classified as M1 and M2 phenotype based on the surface receptor they express, the chemokines and cytokines they produce, and their function. M1 macrophages are classically activated macrophages and are pro-inflammatory. In contrast M2 macrophages are alternatively activated and are anti-inflammatory [45–47]. We found an increased number of foamy M2 phenotype like macrophages (distinguished by their increased expression of IL-10, Arg1 and CD163 and reduced expression of iNOS) in the lungs of *M. tb* infected TF^{Δ} mice lungs compared to *M. tb* infected $TF^{fl/fl}$ mice. The *M. tb* pathogen promotes transition of macrophages towards an M2 phenotype to evade host immune responses [48–50]. Our current findings have demonstrated that TF plays an important role in preventing *M. tb* induced macrophage conversion to an M2 like phenotype. It is not known if TF drives the macrophage phenotype towards the pro-inflammatory M1 phenotype in *M. tb* infection. Wingless-type MMTV integration site family member 6 (Wnt6) signaling during an *M. tb* infection disrupts the inflammatory response by macrophages in granulomatous lesions in the lungs, driving M2 like polarization [49], and we speculate that TF may inhibit some of these signaling pathways to prevent M2 polarization during *M. tb* infection.

M. tb-infected macrophages undergo apoptosis to prevent the spread of infection and to eliminate the pathogen [51–54]. IL-10 inhibits the apoptosis of *M. tb* infected murine and human macrophages [34]. *M. tb*-infected TF^{Δ} mice have more foamy IL-10+ macrophages in their lung lesions (Fig. 3) and these are known to be less apoptotic [14–16]. We found that lack of TF expression in *M. tb*-infected human MDMs and mouse macrophages caused higher MMP levels and reduced apoptosis. We also found that IL-10 siRNA enhanced the loss of $\Delta\Psi m$ and apoptosis in *M. tb* infected human MDMs. Endogenous IL-10 is known to prevent apoptosis in macrophages that are infected with bacteria and down regulate reactive oxygen species production which causes the loss of MMP [55–57]. Loss of $\Delta\Psi m$ is one of the mechanisms involved in apoptosis, and it leads to the release of cytochrome c and

enhanced caspase activity during apoptosis [17, 58, 59]. In the current study, we found that a deficiency of TF in myeloid cells was associated with enhanced IL-10 production, a reduction in the loss of $\Delta\Psi m$, reduced apoptosis and increased *M. tb* growth in macrophages. TF is known to be involved in cell survival signaling, but the outcome of this signaling depends on the cell type and the signaling pathways involved. TF inhibits apoptosis in cancer cells and various signaling pathways such as the PI3-kinase/c-Akt pathway and Jak/STAT5 pathways are involved in the TF mediated inhibition of apoptosis [6, 60–62]. In contrast, TF in HaCaT cells enhances apoptosis through PAR-2-mediated phosphorylation of the cAMP response-element binding protein [3, 63]. In the current study, we found that TF siRNA inhibits apoptosis of *M. tb*-infected human MDMs and that macrophages from *M. tb*-infected TF^{Δ} mice are less apoptotic than *M. tb*-infected $TF^{fl/fl}$ macrophages. Combined, these results demonstrate that TF has a pro-apoptotic role in *M. tb* infection by which it controls bacterial growth and the spread of infection. Our results suggest that TF enhances apoptosis in *M. tb*-infected macrophages by reducing IL-10 production and acting through mitochondrial signaling pathways.

We found increased inflammatory lesions (Fig. 3) and CD4+ and CD8+ cells in the lungs of *M. tb* infected TF^{Δ} mouse lungs compared to *M. tb* infected $TF^{fl/fl}$ mice (Fig. 5). Real-time PCR analyses demonstrated that this increased inflammation was not due to increased IFN-γ or IL-17 production (Fig. 5). MMPs, mainly MMP-2 and MMP-9, are key mediators of inflammation in pulmonary tuberculosis infection [20, 64]. Immunohistochemical analysis of *M. tb* infected TF^{Δ} mouse lungs indicated that MMP-2 and MMP-9 mediated inflammation is responsible for the increased inflammation in *M. tb* infected TF^{Δ} mouse lungs (Fig. 6). MMPs are proteases that degrade extracellular matrix macromolecules, including the structural fibrils of the lung [65]. Extracellular matrix degradation is critical for the successful establishment of infection by *M. tb* [20]. In a zebrafish model of *M. marinum* infection, a lack of MMP-9 expression led to small granulomas and decreased dissemination [66]. Tuberculosis patients exhibit abundant MMP-9 and *M. tb*-infected murine macrophages produce MMP-9 [67–69]. In *M. tb* infection, multiple cellular pathways are involved in MMP production [20]. In many disease conditions, there is a direct correlation between TF expression and the expression of MMPs expression, but we are aware of no previous study that has focused on the interactions between TF and MMPs during the early stages of infection. It is not clear how TF regulates MMP-2 and MMP-9 expression, but one possibility is that the lack of TF expression in *M. tb* infected macrophages leads to transcriptional deregulation or decreased production of endogenous inhibitors, such as tissue inhibitors of metalloproteinases (TIMPs), and this may be responsible for increased MMP-2 and MMP-9 expression [65]. Another possibility is that the lack of TF and the increased *M. tb* growth in macrophages leads to excess production of *M. tb* proteins such as ESAT-6, which are known to induce MMP-9 expression in epithelial cells [66]. While we have not determined the source for MMP-2 and MMP-9, one potential explanation is that lack of TF expression can lead to enhanced infiltration by neutrophils, which are known to produce MMP-2 and MMP-9 [70, 71]. Our study suggests that, during the early phases of the immune response to intracellular pathogens, TF may inhibit the excessive inflammation normally mediated by MMPs to prevent the dissemination of the pathogen and to favor the development of a Th1 response.

The interactions between TF and clotting factor VII/VIIa (FVIIa) lead to the generation of thrombin which converts fibrinogen to fibrin [72]. In acute lung injury and pneumonia, blockade of TF expression inhibits fibrin deposition [8, 73]. Fibrin deposition in the lung is essential for cell trafficking and serves as a structural barrier to various infections [65]. Binding of FVIIa to TF augments the pro-inflammatory functions of macrophages and enhances the production of reactive oxygen species and the expression of major histocompatibility complex class II and cell adhesion molecules [74]. Mice expressing low levels of TF produce less IL-6 and survive for longer periods of time in response to endotoxins compared to control mice [75]. In a number of infections, TF appears to play be a significant outcome determinant. In an E. coli infection, blocking the TF-FVIIa complex decreases intra-alveolar inflammation and fibrin deposition, indicating its essential role in lung injury [73]. Mice infected with *Streptococcus pneumoniae* had increased TF expression and fibrin deposits in their lungs with increased thrombin-antithrombin complexes [76]. The containment and resolution of *Plasmodium* falciparum placental infection was associated with TF mediated inflammation, and fibrin deposition [77]. In *Yersinia pestis* infection, fibrin is an essential component of T cell–mediated defense [78] and infected mice expressing a low level of TF had increased mortality similar to that of fibrinogen-deficient mice [79]. Similar to our study, in *Yersinia enterocolitica* infection, low TF expression enhances IL-10 mRNA in mice [79]. In contrast, in *Plasmodium falciparum* infected placentas macrophages accumulate and express TF which causes the accumulation of fibrin and retarded placental growth and low birth weight [77]. In a similar vein, tuberculosis granulomas are surrounded by fibrin and fibrinogen, which are important for the organization and formation of granulomatous tissue [79, 80]. As expected, we observed decreased levels of fibrin deposition in the lungs of *M. tb* infected TF^{Δ} mice and reduced dissemination of the disease. We also observed an increased production of MMP-2 and MMP-9 which are known to degrade fibrin [65]. Our results suggest that increased production of MMP-2 and MMP-9 may contribute to reduced fibrin deposition in the lungs of *M. tb* infected TF-deficient mice, apart from impaired TF-mediated initiation of local coagulation.

In summary, by using TF^{Δ} mice, as a murine model of *M. tb* infection and human MDMs, we provide the first evidence that TF produced by macrophages contributes to effective immunity against *M. tb* infection. The further delineation of the mechanisms by which TF optimizes immune responses against *M. tb* may facilitate the development of vaccines against this *organism* and other intracellular pathogens. Our results implicate TF in the pathogenesis of organism containment and in the progression of early lung injury following pulmonary *M. tb* infection.

Materials and Methods

Animals

Specific-pathogen-free 4- to 6-week-old female wild-type C57BL/6 mice were purchased from the Jackson Laboratory and housed at the animal facility of University of Texas Health Science Center at Tyler. Mice lacking the TF gene in myeloid cells (TF^{Δ} mice) and their respective controls ($TF^{fl/fl}$) were generated as described previously [81]. All animal

experiments were approved by The Institutional Animal Care and Use Committee of the University of Texas Health Science Center at Tyler.

Blood donors

Blood was obtained from 22 healthy donors. All studies were approved by the Institutional Review Board of the University of Texas Health Science Center at Tyler and written informed consent was provided by all study participants. For the studies performed at the NIH laboratories, peripheral blood mononuclear cells were isolated from blood obtained from the NIH clinical center blood bank.

Antibodies and other reagents

FITC anti-CD4 (clone GK1.5, Biolegend), FITC anti-CD8 (Clone 53–6.7, Biolegend), FITC anti-CD14 (Clone 61D3, eBiosciences), qdot605 anti-CD14 (clone Tük4, Invitrogen), V450 anti-CD2 (clone RPA-2.10, eBioscience), anti-CD3 (clone UCHT1, eBioscience), anti-CD19 (clone HIB19, eBioscience), anti-CD20 (clone 2H7, eBioscience), anti-CD56 (clone B159, eBioscience), PE-Cy7 anti-CD16 (clone 3G8, Biolegend), APC-Cy7 anti-HLA-DR (clone L243, BD biosciences), PE anti-CD142/TF (clone HTF-1,eBioscience) and PerCP-Cy5.5 anti-TNF-α (clone MAb11, eBioscience) were used for flow cytometry, γ-irradiated *M. tb* H37Rv and Ag85a was obtained from BEI Resources.

Isolation of human monocytes and mouse peritoneal and alveolar macrophages

Human PBMC were isolated by differential centrifugation using Ficoll-Paque (Amersham Pharmacia Biotech). $CD14^+$ monocytes were isolated with magnetic beads conjugated to anti-CD14 (Miltenyi Biotec), and positively selected cells were >97% $CD14^+$ as measured by flow cytometry. Mouse bronchoalveolar lavage (BAL) cells and peritoneal exudate macrophages (PEMs) were isolated as previously described [82, 83].

Infection of macrophages with M. tuberculosis H37Rv

Human $CD14^+$ monocytes (1.5×10^6/well) were plated in 12-well plates (BD Biosciences Labware) in 1 ml of antibiotic-free RPMI 1640 containing 10% heat-inactivated human serum. Monocytes were incubated at 37°C in a humidified 5% CO_2 atmosphere for 4 days to allow differentiation to macrophages (MDMs). Mouse PEMs or alveolar macrophages were plated in 12-well plates immediately after isolation and washed after 90 minutes to remove non-adherent cells. Human MDMs or mouse PEMs or alveolar macrophages were infected with *M. tuberculosis* H37Rv at an multiplicity of infection (MOI) of 1:2.5, (2.5 *M. tb* to one MDM) as previously described [84]. This MOI was selected based on the viability of MDMs at different MOIs for up to 7 days post infection. More than 90% of the MDMs were viable at this MOI. Cells were incubated for 2 h at 37°C in a humidified 5% CO_2 atmosphere, washed to remove extracellular bacilli, and cultured in RPMI 1640 containing 10% heat-inactivated human serum.

To quantify the intracellular growth of *M. tb* H37Rv, infected macrophages were cultured for 5 or 7 d, after which the supernatant was aspirated and the macrophages were lysed. Bacterial suspensions in cell lysates were ultrasonically dispersed, serially diluted, and plated in triplicate on 7H10 agar. The number of colonies was counted after 3 weeks.

Stimulation of human PBMC with γ-irradiated M. tb

Human PBMC (1×10^6/well) were plated in 96-well plates in 200μl of antibiotic-free RPMI 1640 containing with 10% heat inactivated human AB serum and 5μg/ml brefeldin-A (Sigma-Aldrich, St. Louis, MO) in the absence or presence of 100 μg/ml of γ-irradiated *M. tb* for 6 hours at 37°C in 5% CO2. Cells were washed and stained with Live/Dead fixable blue dead cell stain (Life Technologies) for 20 minutes at room temperature (RT) then washed with 1% PBS/BSA and stained with antibodies for extracellular surface markers for 1h at RT. Cells were then fixed and permeabilized (Foxp3/ Transcription Factor Staining Buffer Set, eBioscience) overnight at 4°C. After permeabilization, cells were stained for intracellular markers for 1hr at RT. Data were acquired on a BD LSR II flow cytometer (BD Biosciences). All compensation and gating analysis were performed using FlowJo 9.6.3 (TreeStar, Ashland, OR).

Aerosol infection of mice with M. tb H37Rv

Before infecting mice with *M. tb* H37Rv, bacteria were grown in liquid medium to mid-log phase and then frozen in aliquots at −70°C. Bacterial counts were determined by plating on 7H10 agar, supplemented with Oleic Albumin Dextrose Catalase (OADC). For infection, bacterial stocks were diluted in 10 ml of normal saline to 0.5×10^6 CFU; colony forming units/ml, 1×10^6 CFU/ml, 2×10^6 CFU/ml and 4×10^6 CFU/ml and placed in a nebulizer in an aerosol exposure chamber, that was made to order by the University of Wisconsin. In preliminary studies, groups of three mice were exposed to 15 min of aerosol at each concentration, and after 24 h, mice were sacrificed and homogenized lungs were plated on 7H11 agar plates supplemented with OADC. CFU were counted after 14–22 days of incubation at 37°C [85]. For further studies, we selected the concentration that deposited ∼75–100 bacteria in the lungs during aerosol infection.

Real-time PCR for quantification

Total RNA was extracted from MDMs, PEMs or lung cells as described previously [13]. Total RNA was reverse transcribed, using a Clone AMV First-Strand cDNA synthesis kit (Life Technologies). Real-time PCR was performed using the QuantiTect SYBR Green PCR kit (Qiagen) in a sealed 96-well microtiter plate (Applied Biosystems) on a spectrofluorometric thermal cycler (7700 PRISM; Applied Biosystems). PCR reactions were performed in triplicate as follows: 95°C for 10 min, and 45 cycles of 95°C for 15 s, 60°C for 30 s, and 72°C for 30 s. All samples were normalized to the amount of β-actin/GAPDH transcript present in each sample.

The primers that were used in the study are listed in Table I.

siRNA transfection

Human MDMs were transfected with siRNA for TF or control siRNA, using transfection reagents (all from Santa Cruz Biotechnology). The efficiency of siRNA knockdown was measured by real-time PCR of TF mRNA expression. Briefly, 10^6 $CD14^+$ MDMs were resuspended in 500 μl of transfection medium, and transfected with siRNA (6 pmoles). After 6 h, an additional 250 μl of 2X RPMI complete medium was added and cells were cultured

overnight in a 24-well plate. The next day MDMs were infected with H37Rv, as outlined above, and after 3 days culture supernatants were collected and IL-10 production was measured by ELISA and apoptosis was determined as described below.

Measurement of apoptosis of M. tb- infected macrophages

Apoptosis of *M. tb* infected mouse PEMs, mouse lung alveolar cells and human MDMs transfected with a TF siRNA was measured using an APO-Direct TUNEL kit. Briefly, human MDMs and mouse PEMs were infected with *M. tb* H37Rv at a MOI of 2.5:1. Some MDMs were transfected with TF siRNA or control siRNA. After 72 h, cells were isolated using trypsin-EDTA and fixed in 1% paraformaldehyde and 70% ethanol in PBS. Freshly isolated alveolar macrophages from *M. tb* infected mouse were directly fixed in 1% paraformaldehyde and 70% ethanol in PBS. After an overnight incubation at −20°C, cells were washed in washing buffer, resuspended in 50 μl of DNA labelling solution (provided in the kit) and incubated at 37°C. After 60 minutes, cells were washed twice in rinsing buffer and 500 ul of propidium iodide/RNAse A solution was then added followed by incubation in the dark. After 30 minutes, cells were analyzed by flow cytometry [86].

Immunohistochemistry

Immunostaining of lung sections using antibodies against IL-17 (Bioss), IFN-γ (Bioss), IL-10 (Abcam), MMP-2 (Abcam), MMP-9 (Origene) and fibrin/fibrinogen (Abcam) on paraffin fixed thin sections was performed following the manufacturer's instructions as previously described with some modifications [87, 88]. Unstained sections of the formalin fixed lung tissue from paraffin blocks were first deparaffinized and then subjected to antigen retrieval using a citrate buffer at 95°C as previously described [87, 88]. Endogenous peroxidase was blocked with 3% H_2O_2 in methanol. Slides were incubated in 3% BSA in TBS for two min after which primary antibodies were added at predetermined dilutions in TBS-Tween + 1% BSA for 1 hr at 25 °C, and then washed in TBS-T for 15 min 3X. IL-10, MMP 2 and 9 and fibrin (fibrinogen) antigen were detected using immunohistochemistry (IHC) and the Fast Red (BioGenex) chromogen as previously described. The same sections were also used for H & E staining to identify foamy macrophages. Two investigators independently assessed the immunohistochemical readouts using morphometric analyses, as we have previously described [89]. The Histology scores (H-scores) were performed according to the method described by Pirker et al [90]. Briefly, the percentage of cells with different staining intensities were determined by visual assessment and assigned a score for staining intensity (1+ for light staining, 2+ for intermediate staining and 3+ for dark staining) using an immunohistochemistry (IHC) ImageJ profiler. The H score was calculated using the formula 1 × (% of 1 + cells) + 2 × (% of 2 + cells) + 3 × (% of 3 + cells). The percentage of IL-10 positive cells was assessed in ten high-power fields (hpf) per lung.

Measurement of mitochondrial membrane potential (ΔΨm)

The mitochondrial membrane potential (ΔΨm) of the above described cultured cells was measured using a kit (Trevigen) according to manufacturer's instructions. The kit uses a unique cationic dye (5,5'6,6'-tetrachloro-1,1',3, 3'-tetraethylbenzimidazolyl- carbocyanine iodide) to detect the loss of ΔΨm. The dye readily enters cells and fluoresces brightly red in

its multimeric form within healthy mitochondria. In apoptotic cells, the mitochondrial membrane potential collapses, and the dye cannot accumulate within the mitochondria as measured by flow cytometry.

Statistical analysis

Results are shown as the mean ± SE. The Student's *t*-test was used to compare two sets of data and ANOVA followed by a Bonferroni test was used to compare multiple variable groups.

Supplementary Material

Refer to Web version on PubMed Central for supplementary material.

Acknowledgement

This work was supported by grants from the National Institutes of Health (AI054629, AI073612 and A1085135) and CRDF-Global to R.V, and the Cain Foundation for Infectious Disease Research, and the Department of Pulmonary Immunology. This project has been funded in whole or in part with federal funds from the National Cancer Institute, National Institutes of Health, under Contract No. HHSN261200800001E. The content of this publication does not necessarily reflect the views or policies of the Department of Health and Human Services, nor does mention of trade names, commercial products, or organizations imply endorsement by the U.S. Government. This research was supported [in part] by the National Institute of Allergy and Infectious Diseases.

Abbreviations

TF	Tissue factor
M. tb	*Mycobacterium tuberculosis*
MDMs	Monocyte derived macrophages
MOI	Multiplicity of infection
MMP	Matrix metalloproteases

Reference

1. Chan J, Mehta S, Bharrhan S, Chen Y, Achkar JM, Casadevall A, Flynn J. The role of B cells and humoral immunity in Mycobacterium tuberculosis infection. Semin. Immunol. 2014; 26:588–600. [PubMed: 25458990]
2. Kaufmann SHE, Lange C, Rao M, Balaji KN, Lotze M, Schito M, Zumla AI, et al. Progress in tuberculosis vaccine development and host-directed therapies--a state of the art review. Lancet Respir. Med. 2014; 2:301–320. [PubMed: 24717627]
3. Chu AJ. Tissue factor, blood coagulation, and beyond: an overview. Int. J. Inflamm. 2011; 2011:367284.
4. Mackman N. Role of tissue factor in hemostasis, thrombosis, and vascular development. Arterioscler. Thromb. Vasc. Biol. 2004; 24:1015–1022. [PubMed: 15117736]
5. Mackman N. The many faces of tissue factor. J. Thromb. Haemost. JTH. 2009; 7(Suppl 1):136–139. [PubMed: 19630786]
6. van den Hengel LG, Versteeg HH. Tissue factor signaling: a multi-faceted function in biological processes. Front. Biosci. Sch. Ed. 2011; 3:1500–1510.
7. Lopes-Bezerra LM, Filler SG. Endothelial cells, tissue factor and infectious diseases. Braz. J. Med. Biol. Res. Rev. Bras. Pesqui. Médicas E Biológicas Soc. Bras. Biofísica Al. 2003; 36:987–991.

8. van der Poll T. Tissue factor as an initiator of coagulation and inflammation in the lung. Crit. Care Lond. Engl. 2008; 12(Suppl 6):S3.
9. Tucker T, Idell S. Plasminogen-plasmin system in the pathogenesis and treatment of lung and pleural injury. Semin. Thromb. Hemost. 2013; 39:373–381. [PubMed: 23504608]
10. Kothari H, Rao LVM, Vankayalapati R, Pendurthi UR. Mycobacterium tuberculosis infection and tissue factor expression in macrophages. PloS One. 2012; 7:e45700. [PubMed: 23029190]
11. Kothari H, Keshava S, Vatsyayan R, Mackman N, Rao LVM, Pendurthi UR. Role of tissue factor in Mycobacterium tuberculosis-induced inflammation and disease pathogenesis. PloS One. 2014; 9:e114141. [PubMed: 25462128]
12. Redford PS, Murray PJ, O'Garra A. The role of IL-10 in immune regulation during M. tuberculosis infection. Mucosal Immunol. 2011; 4:261–270. [PubMed: 21451501]
13. Dhiman R, Bandaru A, Barnes PF, Saha S, Tvinnereim A, Nayak RC, Paidipally P, et al. c-Maf-dependent growth of Mycobacterium tuberculosis in a CD14(hi) subpopulation of monocyte-derived macrophages. J. Immunol. Baltim. Md 1950. 2011; 186:1638–1645.
14. Junqueira-Kipnis AP, Kipnis A, Henao Tamayo M, Harton M, Gonzalez Juarrero M, Basaraba RJ, Orme IM. Interleukin-10 production by lung macrophages in CBA xid mutant mice infected with Mycobacterium tuberculosis. Immunology. 2005; 115:246–252. [PubMed: 15885131]
15. Peyron P, Vaubourgeix J, Poquet Y, Levillain F, Botanch C, Bardou F, Daffé M, et al. Foamy macrophages from tuberculous patients' granulomas constitute a nutrient-rich reservoir for M. tuberculosis persistence. PLoS Pathog. 2008; 4:e1000204. [PubMed: 19002241]
16. Russell DG, Cardona P-J, Kim M-J, Allain S, Altare F. Foamy macrophages and the progression of the human tuberculosis granuloma. Nat. Immunol. 2009; 10:943–948. [PubMed: 19692995]
17. Gottlieb E, Armour SM, Harris MH, Thompson CB. Mitochondrial membrane potential regulates matrix configuration and cytochrome c release during apoptosis. Cell Death Differ. 2003; 10:709–717. [PubMed: 12761579]
18. Jaworska J, Coulombe F, Downey J, Tzelepis F, Shalaby K, Tattoli I, Berube J, et al. NLRX1 prevents mitochondrial induced apoptosis and enhances macrophage antiviral immunity by interacting with influenza virus PB1-F2 protein. Proc. Natl. Acad. Sci. U. S. A. 2014; 111:E2110–E2119. [PubMed: 24799673]
19. Matsuo J, Nakamura S, Ito A, Yamazaki T, Ishida K, Hayashi Y, Yoshida M, et al. Protochlamydia induces apoptosis of human HEp-2 cells through mitochondrial dysfunction mediated by chlamydial protease-like activity factor. PloS One. 2013; 8:e56005. [PubMed: 23409113]
20. Elkington PT, Ugarte-Gil CA, Friedland JS. Matrix metalloproteinases in tuberculosis. Eur. Respir. J. 2011; 38:456–464. [PubMed: 21659415]
21. Elkington PT, D'Armiento JM, Friedland JS. Tuberculosis immunopathology: the neglected role of extracellular matrix destruction. Sci. Transl. Med. 2011; 3:71ps6.
22. Levi M, Schultz M, van der Poll T. Disseminated intravascular coagulation in infectious disease. Semin. Thromb. Hemost. 2010; 36:367–377. [PubMed: 20614389]
23. Levi M, van der Poll T, Schultz M. Infection and inflammation as risk factors for thrombosis and atherosclerosis. Semin. Thromb. Hemost. 2012; 38:506–514. [PubMed: 22399308]
24. Pawlinski R, Pedersen B, Schabbauer G, Tencati M, Holscher T, Boisvert W, Andrade-Gordon P, et al. Role of tissue factor and protease-activated receptors in a mouse model of endotoxemia. Blood. 2004; 103:1342–1347. [PubMed: 14576054]
25. Van Den Boogaard FE, Brands X, Schultz MJ, Levi M, Roelofs JJTH, Van 't Veer C, Van Der Poll T. Recombinant human tissue factor pathway inhibitor exerts anticoagulant, anti-inflammatory and antimicrobial effects in murine pneumococcal pneumonia. J. Thromb. Haemost. JTH. 2011; 9:122–132. [PubMed: 21029363]
26. Pawlinski R, Pedersen B, Erlich J, Mackman N. Role of tissue factor in haemostasis, thrombosis, angiogenesis and inflammation: lessons from low tissue factor mice. Thromb. Haemost. 2004; 92:444–450. [PubMed: 15351839]
27. Gabryšová L, Howes A, Saraiva M, O'Garra A. The regulation of IL-10 expression. Curr. Top. Microbiol. Immunol. 2014; 380:157–190. [PubMed: 25004818]
28. O'Garra A, Murphy KM. From IL-10 to IL-12: how pathogens and their products stimulate APCs to induce T(H)1 development. Nat. Immunol. 2009; 10:929–932. [PubMed: 19692989]

29. O'Garra A, Barrat FJ, Castro AG, Vicari A, Hawrylowicz C. Strategies for use of IL-10 or its antagonists in human disease. Immunol. Rev. 2008; 223:114–131. [PubMed: 18613832]
30. Redford PS, Boonstra A, Read S, Pitt J, Graham C, Stavropoulos E, Bancroft GJ, et al. Enhanced protection to Mycobacterium tuberculosis infection in IL-10-deficient mice is accompanied by early and enhanced Th1 responses in the lung. Eur. J. Immunol. 2010; 40:2200–2210. [PubMed: 20518032]
31. Turner J, Gonzalez-Juarrero M, Ellis DL, Basaraba RJ, Kipnis A, Orme IM, Cooper AM. In vivo IL-10 production reactivates chronic pulmonary tuberculosis in C57BL/6 mice. J. Immunol. Baltim. Md 1950. 2002; 169:6343–6351.
32. Brockman MA, Kwon DS, Tighe DP, Pavlik DF, Rosato PC, Sela J, Porichis F, et al. IL-10 is up-regulated in multiple cell types during viremic HIV infection and reversibly inhibits virus-specific T cells. Blood. 2009; 114:346–356. [PubMed: 19365081]
33. Granelli-Piperno A, Golebiowska A, Trumpfheller C, Siegal FP, Steinman RM. HIV-1-infected monocyte-derived dendritic cells do not undergo maturation but can elicit IL-10 production and T cell regulation. Proc. Natl. Acad. Sci. U. S. A. 2004; 101:7669–7674. [PubMed: 15128934]
34. Rojas M, Olivier M, Gros P, Barrera LF, García LF. TNF-alpha and IL-10 modulate the induction of apoptosis by virulent Mycobacterium tuberculosis in murine macrophages. J. Immunol. Baltim. Md 1950. 1999; 162:6122–6131.
35. Gil DP, León LG, Correa LI, Maya JR, París SC, García LF, Rojas M. Differential induction of apoptosis and necrosis in monocytes from patients with tuberculosis and healthy control subjects. J. Infect. Dis. 2004; 189:2120–2128. [PubMed: 15143481]
36. Veltrop MH, Langermans JA, Thompson J, Bancsi MJ. Interleukin-10 regulates the tissue factor activity of monocytes in an in vitro model of bacterial endocarditis. Infect. Immun. 2001; 69:3197–3202. [PubMed: 11292741]
37. Martinez FO, Gordon S, Locati M, Mantovani A. Transcriptional profiling of the human monocyte-to-macrophage differentiation and polarization: new molecules and patterns of gene expression. J. Immunol. Baltim. Md 1950. 2006; 177:7303–7311.
38. Cao S, Liu J, Song L, Ma X. The protooncogene c-Maf is an essential transcription factor for IL-10 gene expression in macrophages. J. Immunol. Baltim. Md 1950. 2005; 174:3484–3492.
39. Bauquet AT, Jin H, Paterson AM, Mitsdoerffer M, Ho I-C, Sharpe AH, Kuchroo VK. The costimulatory molecule ICOS regulates the expression of c-Maf and IL-21 in the development of follicular T helper cells and TH-17 cells. Nat. Immunol. 2009; 10:167–175. [PubMed: 19098919]
40. Hiramatsu Y, Suto A, Kashiwakuma D, Kanari H, Kagami S, Ikeda K, Hirose K, et al. c-Maf activates the promoter and enhancer of the IL-21 gene, and TGF-beta inhibits c-Maf-induced IL-21 production in CD4+ T cells. J. Leukoc. Biol. 2010; 87:703–712. [PubMed: 20042469]
41. Ho IC, Hodge MR, Rooney JW, Glimcher LH. The proto-oncogene c-maf is responsible for tissue-specific expression of interleukin-4. Cell. 1996; 85:973–983. [PubMed: 8674125]
42. Kim JI, Ho IC, Grusby MJ, Glimcher LH. The transcription factor c-Maf controls the production of interleukin-4 but not other Th2 cytokines. Immunity. 1999; 10:745–751. [PubMed: 10403649]
43. Pot C, Jin H, Awasthi A, Liu SM, Lai C-Y, Madan R, Sharpe AH, et al. Cutting edge: IL-27 induces the transcription factor c-Maf, cytokine IL-21, and the costimulatory receptor ICOS that coordinately act together to promote differentiation of IL-10-producing Tr1 cells. J. Immunol. Baltim. Md 1950. 2009; 183:797–801.
44. Rossi Paccani S, Benagiano M, Capitani N, Zornetta I, Ladant D, Montecucco C, D'Elios MM, et al. The adenylate cyclase toxins of Bacillus anthracis and Bordetella pertussis promote Th2 cell development by shaping T cell antigen receptor signaling. PLoS Pathog. 2009; 5:e1000325. [PubMed: 19266022]
45. Boven LA, Van Meurs M, Van Zwam M, Wierenga-Wolf A, Hintzen RQ, Boot RG, Aerts JM, et al. Myelin-laden macrophages are anti-inflammatory, consistent with foam cells in multiple sclerosis. Brain J. Neurol. 2006; 129:517–526.
46. Mosser DM, Edwards JP. Exploring the full spectrum of macrophage activation. Nat. Rev. Immunol. 2008; 8:958–969. [PubMed: 19029990]
47. Mosser DM, Zhang X. Activation of murine macrophages. Curr. Protoc. Immunol. Ed. John E Coligan Al. 2008; 14:2. Chapter 14:Unit.

48. Raju B, Hoshino Y, Belitskaya-Lévy I, Dawson R, Ress S, Gold JA, Condos R, et al. Gene expression profiles of bronchoalveolar cells in pulmonary TB. Tuberc. Edinb. Scotl. 2008; 88:39–51.
49. Schaale K, Brandenburg J, Kispert A, Leitges M, Ehlers S, Reiling N. Wnt6 is expressed in granulomatous lesions of Mycobacterium tuberculosis-infected mice and is involved in macrophage differentiation and proliferation. J. Immunol. Baltim. Md 1950. 2013; 191:5182–5195.
50. Lugo-Villarino G, Balla KM, Stachura DL, Bañuelos K, Werneck MBF, Traver D. Identification of dendritic antigen-presenting cells in the zebrafish. Proc. Natl. Acad. Sci. U. S. A. 2010; 107:15850–15855. [PubMed: 20733076]
51. Keane J, Shurtleff B, Kornfeld H. TNF-dependent BALB/c murine macrophage apoptosis following Mycobacterium tuberculosis infection inhibits bacillary growth in an IFN-gamma independent manner. Tuberc. Edinb. Scotl. 2002; 82:55–61.
52. Keane J, Remold HG, Kornfeld H. Virulent Mycobacterium tuberculosis strains evade apoptosis of infected alveolar macrophages. J. Immunol. Baltim. Md 1950. 2000; 164:2016–2020.
53. Lee J, Hartman M, Kornfeld H. Macrophage apoptosis in tuberculosis. Yonsei Med. J. 2009; 50:1–11. [PubMed: 19259342]
54. Lee J, Remold HG, Ieong MH, Kornfeld H. Macrophage apoptosis in response to high intracellular burden of Mycobacterium tuberculosis is mediated by a novel caspase-independent pathway. J. Immunol. Baltim. Md 1950. 2006; 176:4267–4274.
55. Arai T, Hiromatsu K, Nishimura H, Kimura Y, Kobayashi N, Ishida H, Nimura Y, et al. Endogenous interleukin 10 prevents apoptosis in macrophages during Salmonella infection. Biochem. Biophys. Res. Commun. 1995; 213:600–607. [PubMed: 7646518]
56. Dang PM-C, Elbim C, Marie J-C, Chiandotto M, Gougerot-Pocidalo M-A, El-Benna J. Anti-inflammatory effect of interleukin-10 on human neutrophil respiratory burst involves inhibition of GM-CSF-induced p47PHOX phosphorylation through a decrease in ERK1/2 activity. FASEB J. Off. Publ. Fed. Am. Soc. Exp. Biol. 2006; 20:1504–1506.
57. Suski JM, Lebiedzinska M, Bonora M, Pinton P, Duszynski J, Wieckowski MR. Relation between mitochondrial membrane potential and ROS formation. Methods Mol. Biol. Clifton NJ. 2012; 810:183–205.
58. de Moissac D, Gurevich RM, Zheng H, Singal PK, Kirshenbaum LA. Caspase activation and mitochondrial cytochrome C release during hypoxia-mediated apoptosis of adult ventricular myocytes. J. Mol. Cell. Cardiol. 2000; 32:53–63. [PubMed: 10652190]
59. Gogvadze V, Orrenius S, Zhivotovsky B. Multiple pathways of cytochrome c release from mitochondria in apoptosis. Biochim. Biophys. Acta. 2006; 1757:639–647. [PubMed: 16678785]
60. Versteeg HH, Spek CA, Slofstra SH, Diks SH, Richel DJ, Peppelenbosch MP. FVIIa:TF induces cell survival via G12/G13-dependent Jak/STAT activation and BclXL production. Circ. Res. 2004; 94:1032–1040. [PubMed: 15016732]
61. Versteeg HH, Spek CA, Richel DJ, Peppelenbosch MP. Coagulation factors VIIa and Xa inhibit apoptosis and anoikis. Oncogene. 2004; 23:410–417. [PubMed: 14724569]
62. Sorensen BB, Rao LVM, Tornehave D, Gammeltoft S, Petersen LC. Antiapoptotic effect of coagulation factor VIIa. Blood. 2003; 102:1708–1715. [PubMed: 12738672]
63. Versteeg HH, Borensztajn KS, Kerver ME, Ruf W, Reitsma PH, Spek CA, Peppelenbosch MP. TF:FVIIa-specific activation of CREB upregulates proapoptotic proteins via protease-activated receptor-2. J. Thromb. Haemost. JTH. 2008; 6:1550–1557. [PubMed: 18647225]
64. Salgame P. MMPs in tuberculosis: granuloma creators and tissue destroyers. J. Clin. Invest. 2011; 121:1686–1688. [PubMed: 21519148]
65. Hotary KB, Yana I, Sabeh F, Li X-Y, Holmbeck K, Birkedal-Hansen H, Allen ED, et al. Matrix metalloproteinases (MMPs) regulate fibrin-invasive activity via MT1-MMP-dependent and -independent processes. J. Exp. Med. 2002; 195:295–308. [PubMed: 11828004]
66. Volkman HE, Pozos TC, Zheng J, Davis JM, Rawls JF, Ramakrishnan L. Tuberculous granuloma induction via interaction of a bacterial secreted protein with host epithelium. Science. 2010; 327:466–469. [PubMed: 20007864]

67. Park KJ, Hwang SC, Sheen SS, Oh YJ, Han JH, Lee KB. Expression of matrix metalloproteinase-9 in pleural effusions of tuberculosis and lung cancer. Respir. Int. Rev. Thorac. Dis. 2005; 72:166–175.
68. Sheen P, O'Kane CM, Chaudhary K, Tovar M, Santillan C, Sosa J, Caviedes L, et al. High MMP-9 activity characterises pleural tuberculosis correlating with granuloma formation. Eur. Respir. J. 2009; 33:134–141. [PubMed: 18715875]
69. Hoheisel G, Sack U, Hui DS, Huse K, Chan KS, Chan KK, Hartwig K, et al. Occurrence of matrix metalloproteinases and tissue inhibitors of metalloproteinases in tuberculous pleuritis. Tuberc. Edinb. Scotl. 2001; 81:203–209.
70. Vlahos R, Wark PAB, Anderson GP, Bozinovski S. Glucocorticosteroids differentially regulate MMP-9 and neutrophil elastase in COPD. PloS One. 2012; 7:e33277. [PubMed: 22413009]
71. Geraghty P, Rogan MP, Greene CM, Boxio RMM, Poiriert T, O'Mahony M, Belaaouaj A, et al. Neutrophil elastase up-regulates cathepsin B and matrix metalloprotease-2 expression. J. Immunol. Baltim. Md 1950. 2007; 178:5871–5878.
72. Nemerson Y. Tissue factor and hemostasis. Blood. 1988; 71:1–8. [PubMed: 3275472]
73. Miller DL, Welty-Wolf K, Carraway MS, Ezban M, Ghio A, Suliman H, Piantadosi CA. Extrinsic coagulation blockade attenuates lung injury and proinflammatory cytokine release after intratracheal lipopolysaccharide. Am. J. Respir. Cell Mol. Biol. 2002; 26:650–658. [PubMed: 12034563]
74. Cunningham MA, Romas P, Hutchinson P, Holdsworth SR, Tipping PG. Tissue factor and factor VIIa receptor/ligand interactions induce proinflammatory effects in macrophages. Blood. 1999; 94:3413–3420. [PubMed: 10552951]
75. Pawlinski R, Mackman N. Tissue factor, coagulation proteases, and protease-activated receptors in endotoxemia and sepsis. Crit. Care Med. 2004; 32:S293–S297. [PubMed: 15118533]
76. Rijneveld AW, Weijer S, Bresser P, Florquin S, Vlasuk GP, Rote WE, Spek CA, et al. Local activation of the tissue factor-factor VIIa pathway in patients with pneumonia and the effect of inhibition of this pathway in murine pneumococcal pneumonia. Crit. Care Med. 2006; 34:1725–1730. [PubMed: 16625114]
77. Imamura T, Sugiyama T, Cuevas LE, Makunde R, Nakamura S. Expression of tissue factor, the clotting initiator, on macrophages in Plasmodium falciparum-infected placentas. J. Infect. Dis. 2002; 186:436–440. [PubMed: 12134244]
78. Luo D, Lin J-S, Parent MA, Mullarky-Kanevsky I, Szaba FM, Kummer LW, Duso DK, et al. Fibrin facilitates both innate and T cell-mediated defense against Yersinia pestis. J. Immunol. Baltim. Md 1950. 2013; 190:4149–4161.
79. Luo D, Szaba FM, Kummer LW, Plow EF, Mackman N, Gailani D, Smiley ST. Protective roles for fibrin, tissue factor, plasminogen activator inhibitor-1, and thrombin activatable fibrinolysis inhibitor, but not factor XI, during defense against the gram-negative bacterium Yersinia enterocolitica. J. Immunol. Baltim. Md 1950. 2011; 187:1866–1876.
80. Turner OC, Basaraba RJ, Orme IM. Immunopathogenesis of pulmonary granulomas in the guinea pig after infection with Mycobacterium tuberculosis. Infect. Immun. 2003; 71:864–871. [PubMed: 12540568]
81. Sakamoto K, Geisel RE, Kim M-J, Wyatt BT, Sellers LB, Smiley ST, Cooper AM, et al. Fibrinogen regulates the cytotoxicity of mycobacterial trehalose dimycolate but is not required for cell recruitment, cytokine response, or control of mycobacterial infection. Infect. Immun. 2010; 78:1004–1011. [PubMed: 20028811]
82. Pawlinski R, Wang J-G, Owens AP, Williams J, Antoniak S, Tencati M, Luther T, et al. Hematopoietic and nonhematopoietic cell tissue factor activates the coagulation cascade in endotoxemic mice. Blood. 2010; 116:806–814. [PubMed: 20410508]
83. Okada S, Hasegawa S, Hasegawa H, Ainai A, Atsuta R, Ikemoto K, Sasaki K, et al. Analysis of bronchoalveolar lavage fluid in a mouse model of bronchial asthma and H1N1 2009 infection. Cytokine. 2013; 63:194–200. [PubMed: 23706975]
84. Zhang X, Goncalves R, Mosser DM. The isolation and characterization of murine macrophages. Curr. Protoc. Immunol. Ed. John E Coligan Al. 2008; 14:1. Chapter 14:Unit.

85. Dhiman R, Indramohan M, Barnes PF, Nayak RC, Paidipally P, Rao LVM, Vankayalapati R. IL-22 produced by human NK cells inhibits growth of Mycobacterium tuberculosis by enhancing phagolysosomal fusion. J. Immunol. Baltim. Md 1950. 2009; 183:6639–6645.

86. Junqueira-Kipnis AP, Kipnis A, Jamieson A, Juarrero MG, Diefenbach A, Raulet DH, Turner J, et al. NK cells respond to pulmonary infection with Mycobacterium tuberculosis, but play a minimal role in protection. J. Immunol. Baltim. Md 1950. 2003; 171:6039–6045.

87. Venkatasubramanian S, Dhiman R, Paidipally P, Cheekatla SS, Tripathi D, Welch E, Tvinnereim AR, et al. A rho GDP dissociation inhibitor produced by apoptotic T-cells inhibits growth of Mycobacterium tuberculosis. PLoS Pathog. 2015; 11:e1004617. [PubMed: 25659138]

88. Jeffers A, Owens S, Koenig K, Quaid B, Pendurthi UR, Rao VM, Idell S, et al. Thrombin down-regulates tissue factor pathway inhibitor expression in a PI3K/nuclear factor-κB-dependent manner in human pleural mesothelial cells. Am. J. Respir. Cell Mol. Biol. 2015; 52:674–682. [PubMed: 25303460]

89. Williams L, Tucker TA, Koenig K, Allen T, Rao LVM, Pendurthi U, Idell S. Tissue factor pathway inhibitor attenuates the progression of malignant pleural mesothelioma in nude mice. Am. J. Respir. Cell Mol. Biol. 2012; 46:173–179. [PubMed: 21852688]

90. Pirker R, Pereira JR, von Pawel J, Krzakowski M, Ramlau R, Park K, de Marinis F, et al. EGFR expression as a predictor of survival for first-line chemotherapy plus cetuximab in patients with advanced non-small-cell lung cancer: analysis of data from the phase 3 FLEX study. Lancet Oncol. 2012; 13:33–42. [PubMed: 22056021]

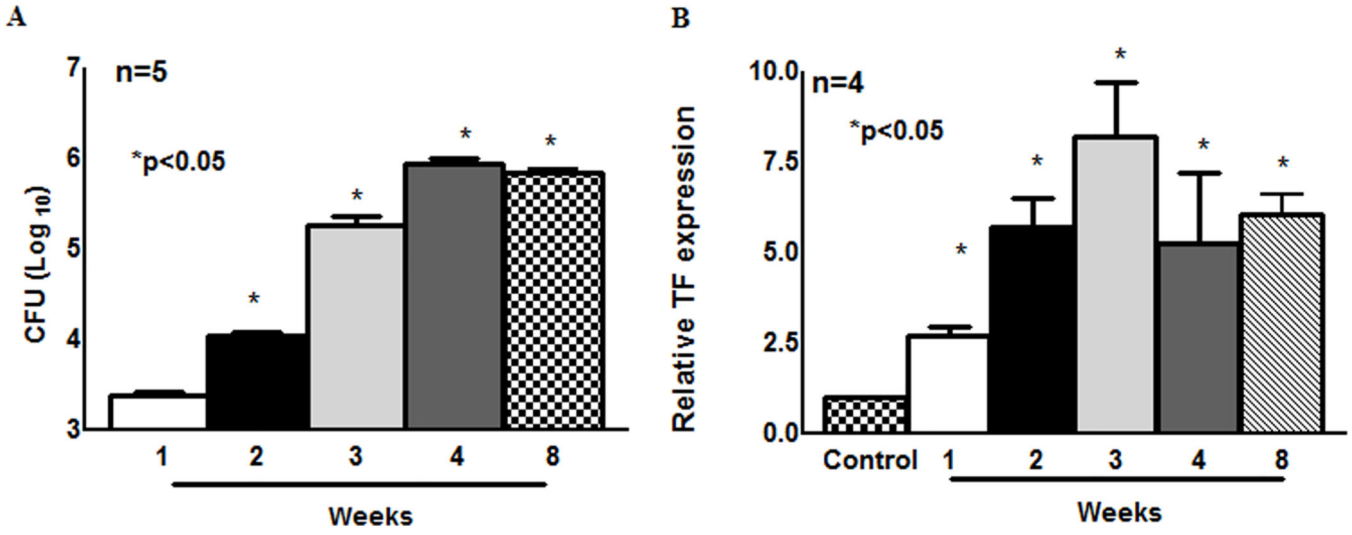

Fig. 1. TF expression and bacterial burden in *M. tb* infected wild type C57BL/6 mice

C57BL/6 mice were infected with ~75–100 CFU of *M. tb* H37Rv, which was delivered by aerosol. At weekly intervals, for up to 4 weeks and at the 8th week, mice in each group were sacrificed, and lung bacterial burden and TF expression were determined by real-time PCR. (**A)** Bacterial burden in lungs. The results are shown as $\log_{10}$ CFU per lung. All data shown as the mean ± SEM and are representative of three independent experiments. Statistical analysis was performed using Student's *t*-test for bacterial counts. (**B)** TF expression in lungs. TF gene expression was assessed by real-time PCR using the SYBR Green system and the ΔΔCT method for relative quantification. Fold changes in gene expression relative to uninfected mice lung are reported. All data are shown as the mean ± SEM and are representative of three independent experiments. Statistical analysis was performed using Student's *t*-test. *p<0.05.

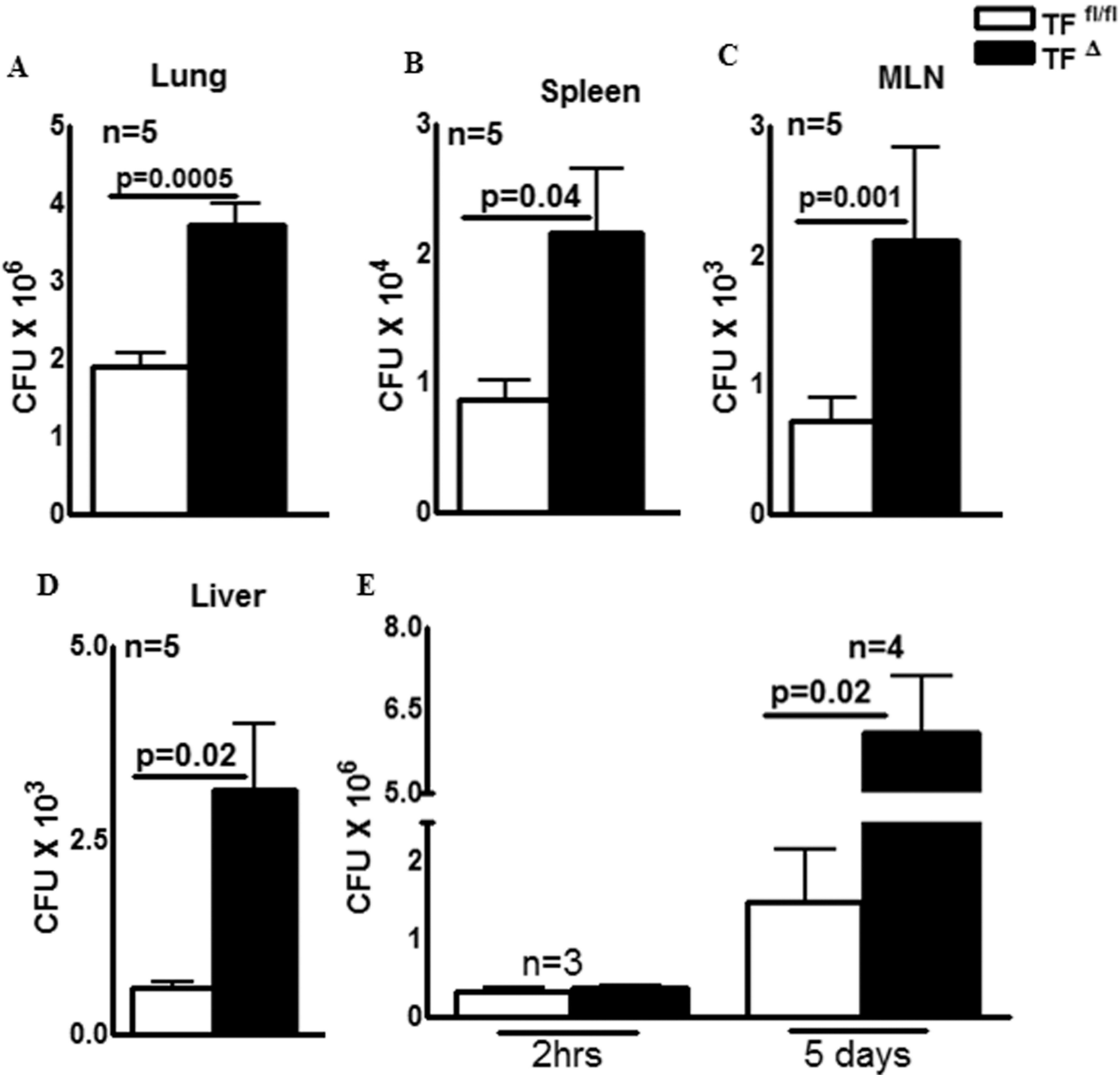

Fig. 2. TF expression by myeloid cells is essential for the optimal control of *M. tb* growth

(A to D) TF^{Δ} mice and $TF^{fl/fl}$ mice both C57BL/6 background were infected with ~75–100 CFU of *M. tb* H37Rv delivered by aerosol. Thirty days after infection, lung, liver, spleen and MLN cells were isolated and bacterial burden was determined. (**A)** Lungs (**B)** Spleen (**C)** MLN and (**D)** Liver. The results are shown in actual bacterial counts. All data shown as the mean ± SEM and are representative of three independent experiments. Statistical analysis was performed using Student's t-test for bacterial counts. (**E)** PEMs from $TF^{fl/fl}$ and TF^{Δ} mice were infected with H37Rv at a MOI of 1:2.5 (2.5 *M. tb* to one PEM). After 2 h, MDMs were washed to remove extracellular bacteria and were cultured. After 2 h and 5 days, CFU were determined. Five days data are shown as the mean ± SEM are

representative of three independent experiments. Statistical analysis was performed using Student's *t*-test.

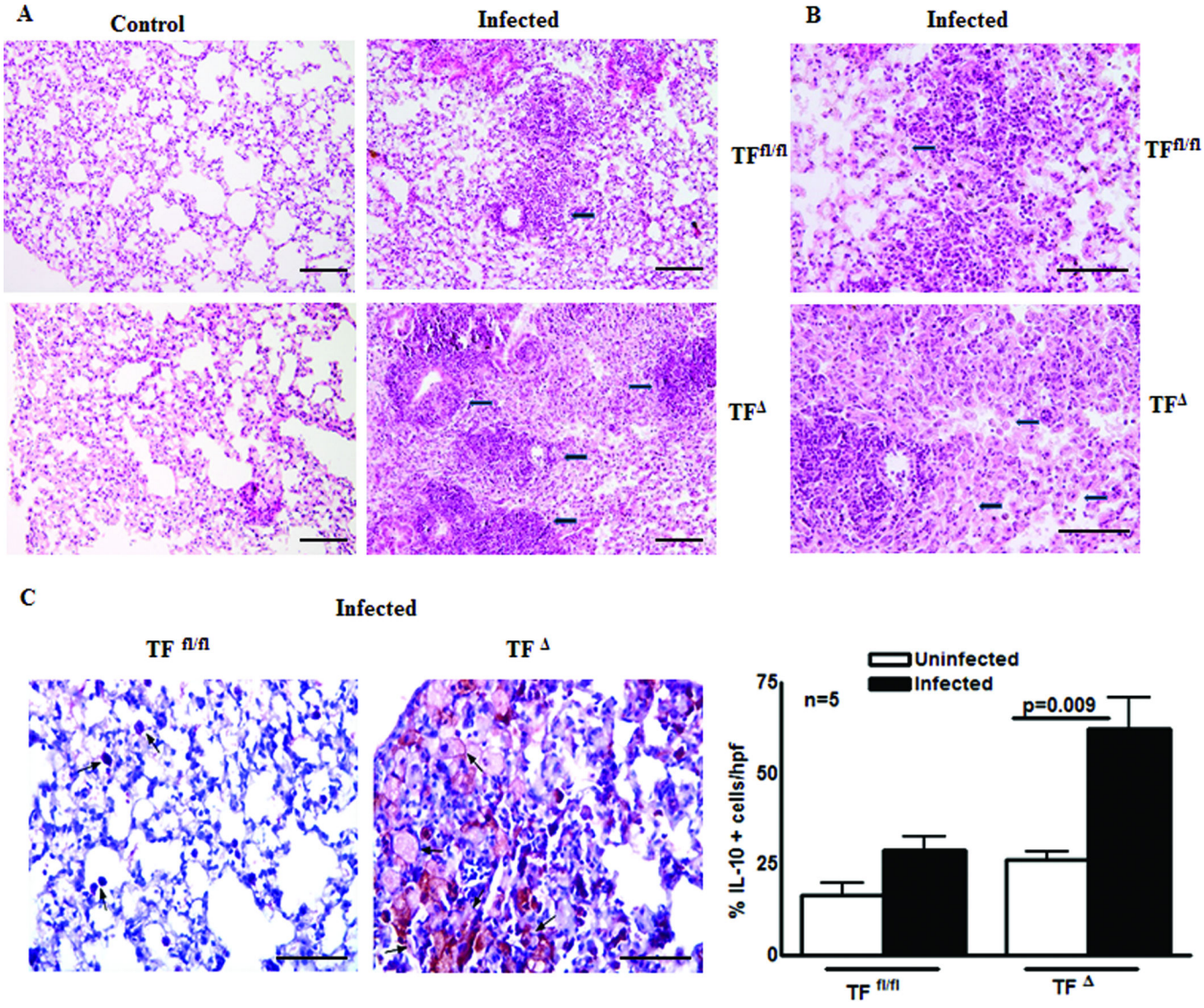

Fig. 3. Immunohistochemical analysis of *M. tb* infected TF^{Δ} and $TF^{fl/fl}$ mice lungs

TF^{Δ} and $TF^{fl/fl}$ mice were infected with ~75–100 CFU of *M. tb* H37Rv delivered by aerosol. After 30 days, lungs from TF^{Δ} and wild type controls and *M. tb* infected mice were isolated, formalin fixed and paraffin-embedded, after which tissue sections were prepared and hematoxylin and eosin staining or Immunohistochemical analysis was performed. (**A)** Histological analysis. Arrow indicates inflammatory regions. Images of multiple fields were obtained at 10X magnification (bar represents 200μm) (**B)** Foamy macrophages. Arrow indicates fomay macrophages surrounding a lymphocytic core structure. Images of multiple fields were obtained at 20X magnification (bar represents 100μm). **C**. Immunohistochemical analysis for IL-10+ foamy macrophages. Photographs are representative of staining patterns. Images of multiple fields were obtained at 20X magnification (bar represents 100μm). All data are shown as the mean ± SEM and are representative of two independent experiment. Statistical analysis was performed using Student's *t*-test.

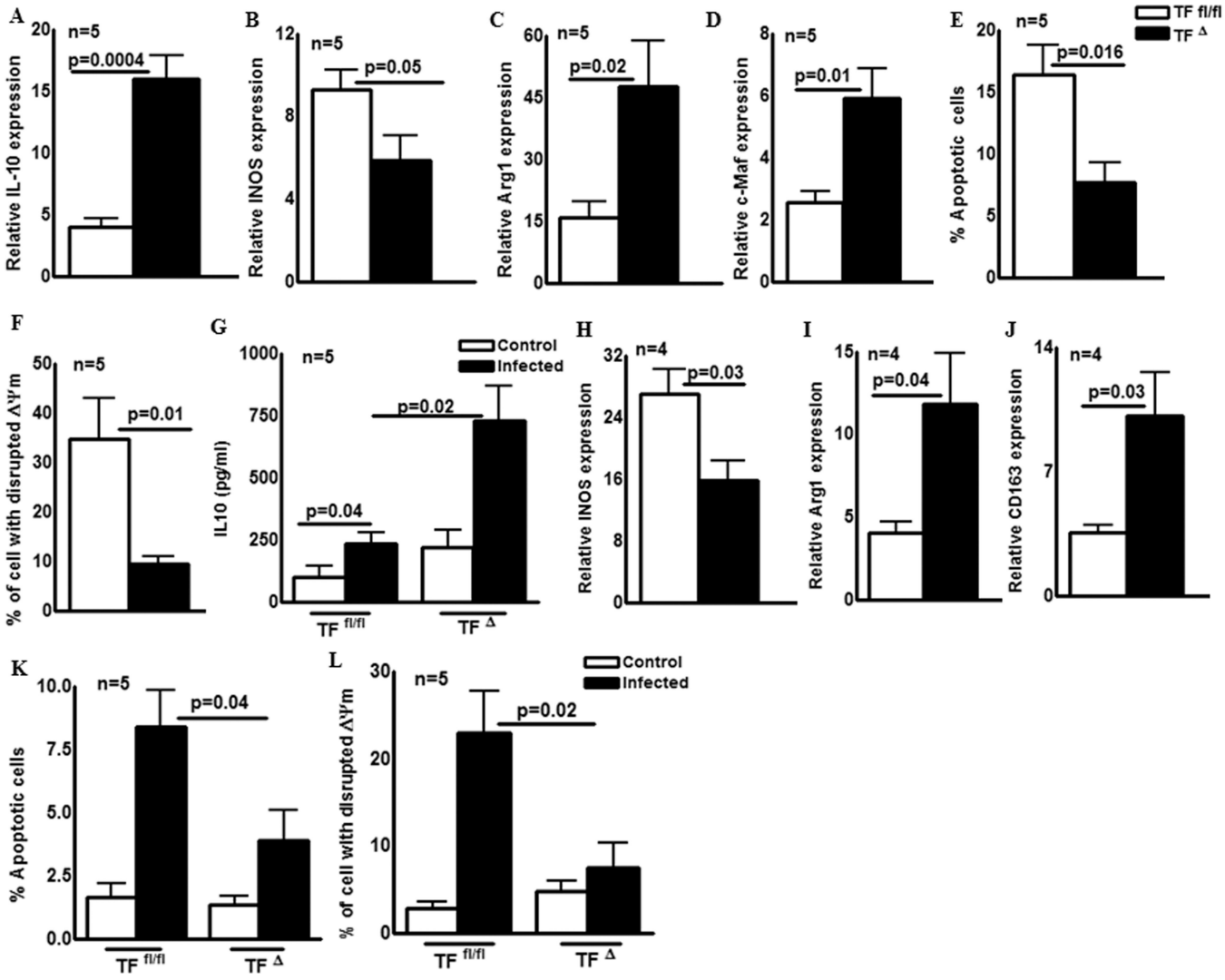

Fig. 4. *M. tb* infected TF$^{\Delta}$ mice lung macrophages produce more IL-10 and are less apoptotic and more polarize towards M2 like phenotype

TF$^{\Delta}$ and wild type mice were infected with ~75–100 CFU of *M. tb* H37Rv delivered by aerosol. Thirty days after infection in lungs (**A)** IL-10, (**B)** iNOS, **(C)** Arg1 and (**D**) c-Maf mRNA expression using real-time PCR was determined. Gene expression was assessed by real-time PCR using the SYBR Green system and the ΔΔCT method for relative quantification. Fold changes in gene expression relative to control uninfected TF$^{\Delta}$ and TF$^{fl/fl}$ mice are shown. (**E)** Lung cells were isolated, and apoptotic cells were identified using a TUNEL assay. (**F)** Lung cells were isolated, and disrupted ΔΨm was determined by using flow cytometry with a kit obtained from Trevigen. All data are shown as mean ± SEM and are representative of five independent experiments. (**G to L)** PEMs from uninfected TF$^{\Delta}$ and TF$^{fl/fl}$ mice were isolated and infected with *M. tb* H37Rv as mentioned in methods section. After 3 days, culture supernatants and cell were collected for RNA isolation. **(G)** IL-10 levels were measured by ELISA. **(H)** iNOS, **(I)** Arg1 and **(J)** CD163 mRNA expression levels were determined using real-time PCR. Gene expression was assessed by real-time PCR using the SYBR Green system and the ΔΔCT method for relative quantification. Fold

changes in gene expression relative to control uninfected TF^{Δ} and $TF^{fl/fl}$ mice PEMs was shown. (**F**) Apoptotic cells were identified using a TUNEL assay. (**G)** Disrupted ΔΨm was determined by flow cytometry using a kit obtained from Trevigen. All statistical analysis was performed using Student's *t*-test. All data are shown as the mean ± SEM and are representative of five independent experiments.

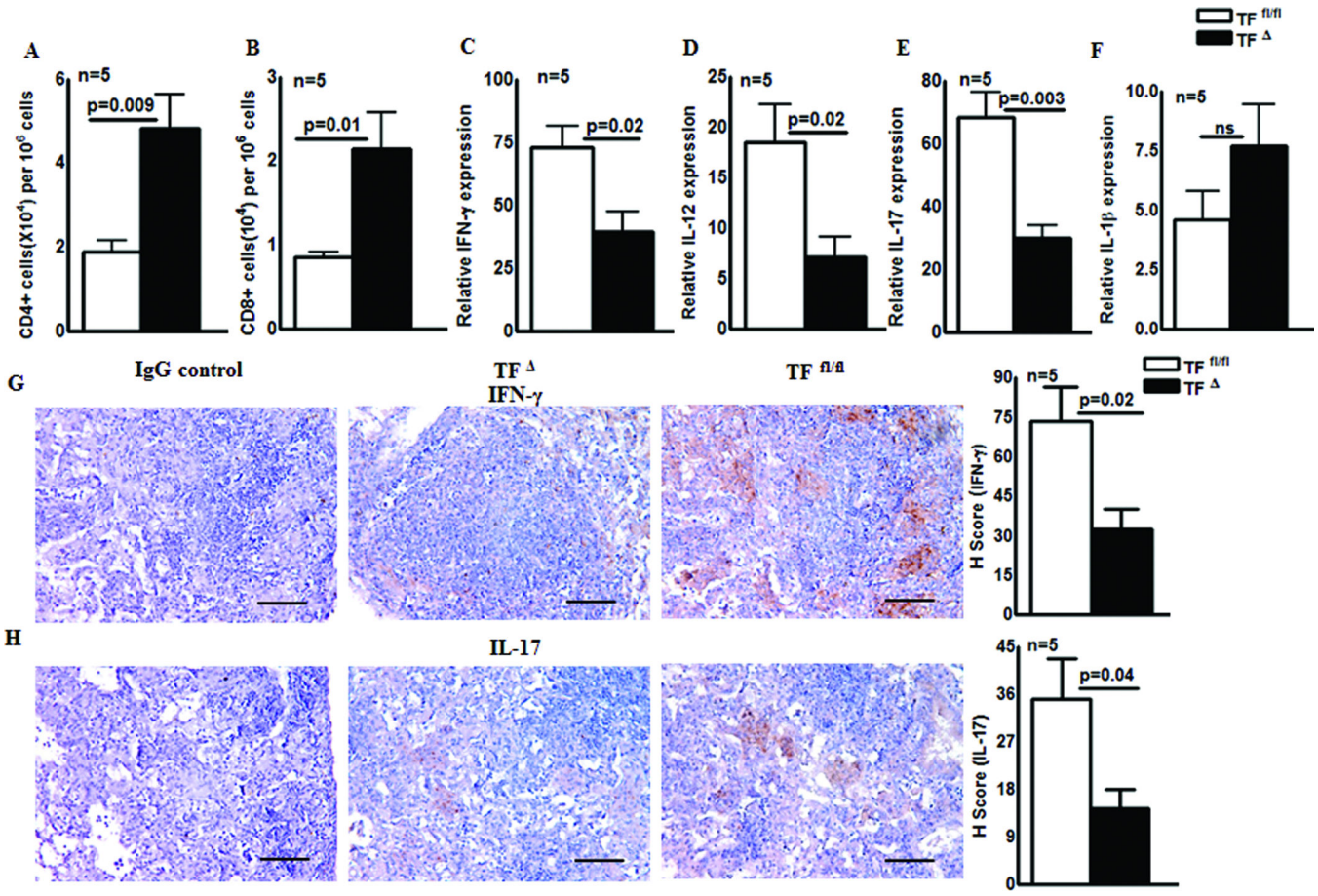

Fig. 5. T-cell numbers and cytokine production by *M. tb* infected TF$^{\Delta}$ and TF$^{fl/fl}$ mice

TF$^{\Delta}$ and **TF$^{fl/fl}$** mice were infected with ~75–100 CFU of *M. tb* H37Rv delivered by aerosol. Thirty days after infection (**A and B)** CD4+ and CD8+ cell numbers were determined by flowcytometry. Statistical analysis was performed using the Student's *t*-test. (**C to F)** IFN-γ, IL-12, IL-17 and IL-1β mRNA expression levels were determined using real-time PCR. Mean values, p values and SEs are shown. Gene expression was assessed by real-time PCR using the SYBR Green system and the ΔΔCT method for relative quantification. Fold changes in gene expression relative to uninfected TF$^{\Delta}$ and TF$^{fl/fl}$ mice lungs are shown. Statistical analysis was performed using the Student's *t*-test. All data are shown as the mean ± SEM and are representative of three independent experiment. **(G and H)**. IFN-γ and IL-17 expression was determined by immunohistochemical analysis. Photographs are representative of the staining patterns of multiple fields and were obtained at 20X magnification (bar represents 100μm). All data are shown as mean ± SEM and are representative of three independent experiment. Statistical analysis was performed using Student's *t*-test.

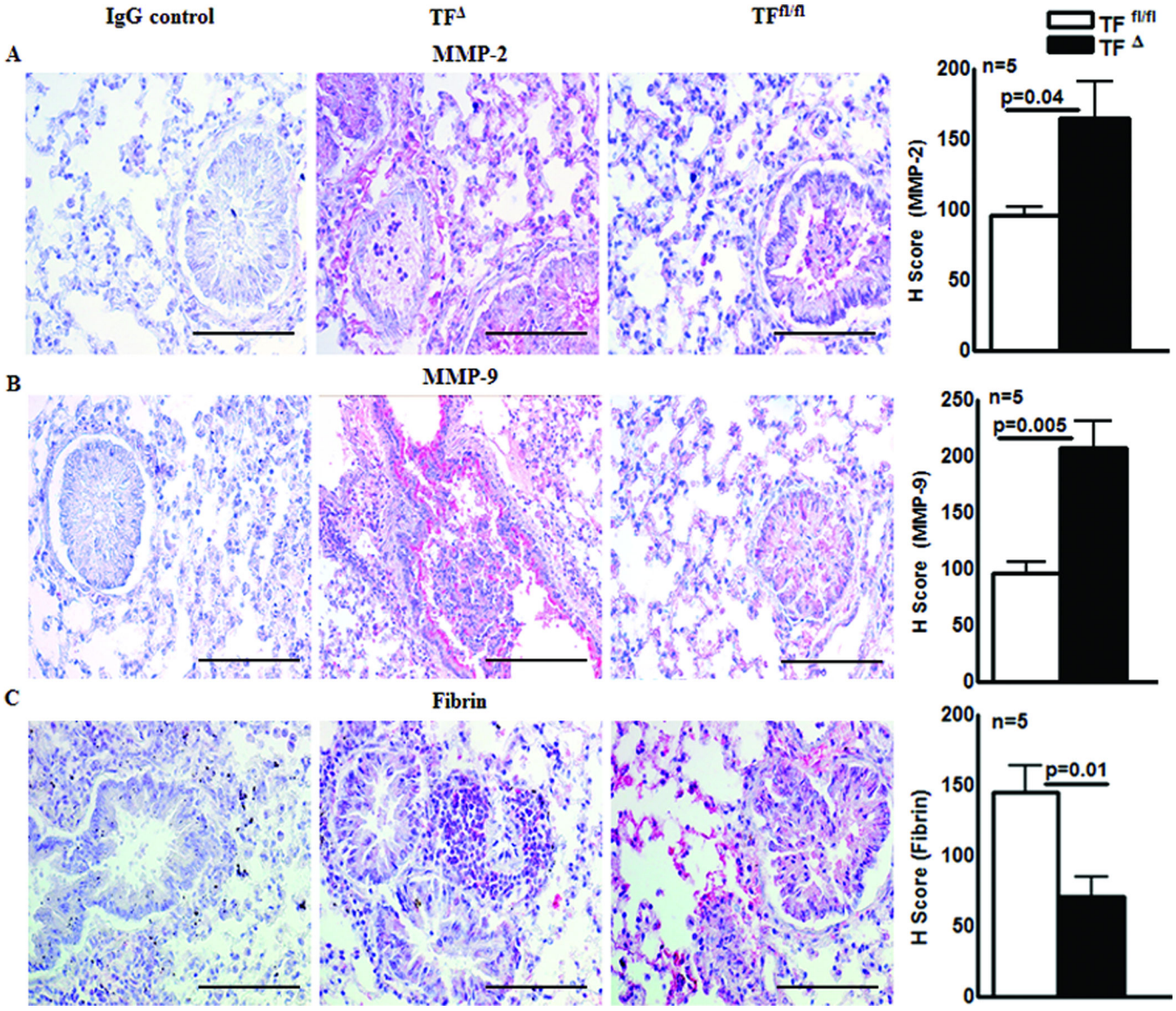

Fig. 6. Expression of MMP-2 and MMP-9 and Fibrin/Fibrinogen deposition in *M. tb* infected TF^{Δ} and $TF^{fl/fl}$ mice

TF^{Δ} and $TF^{fl/fl}$ mice were infected with ~75–100 CFU of *M. tb* H37Rv delivered by aerosol. After 30 days lungs from *M. tb* infected TF^{Δ} and $TF^{fl/fl}$ mice were isolated and tissue sections were prepared after which MMP-2, MMP-9 and fibrin/fibrinogen staining was performed. (**A)** MMP-2 expression. (**B)** MMP-9 expression. (**C)** Fibrin/fibrinogen deposition. Photographs are representative of staining patterns and were taken at 40X magnification. (bar represents 50μm). All data are shown as the mean ± SEM and are representative of three independent experiment. Statistical analysis was performed using the Student's *t*-test.

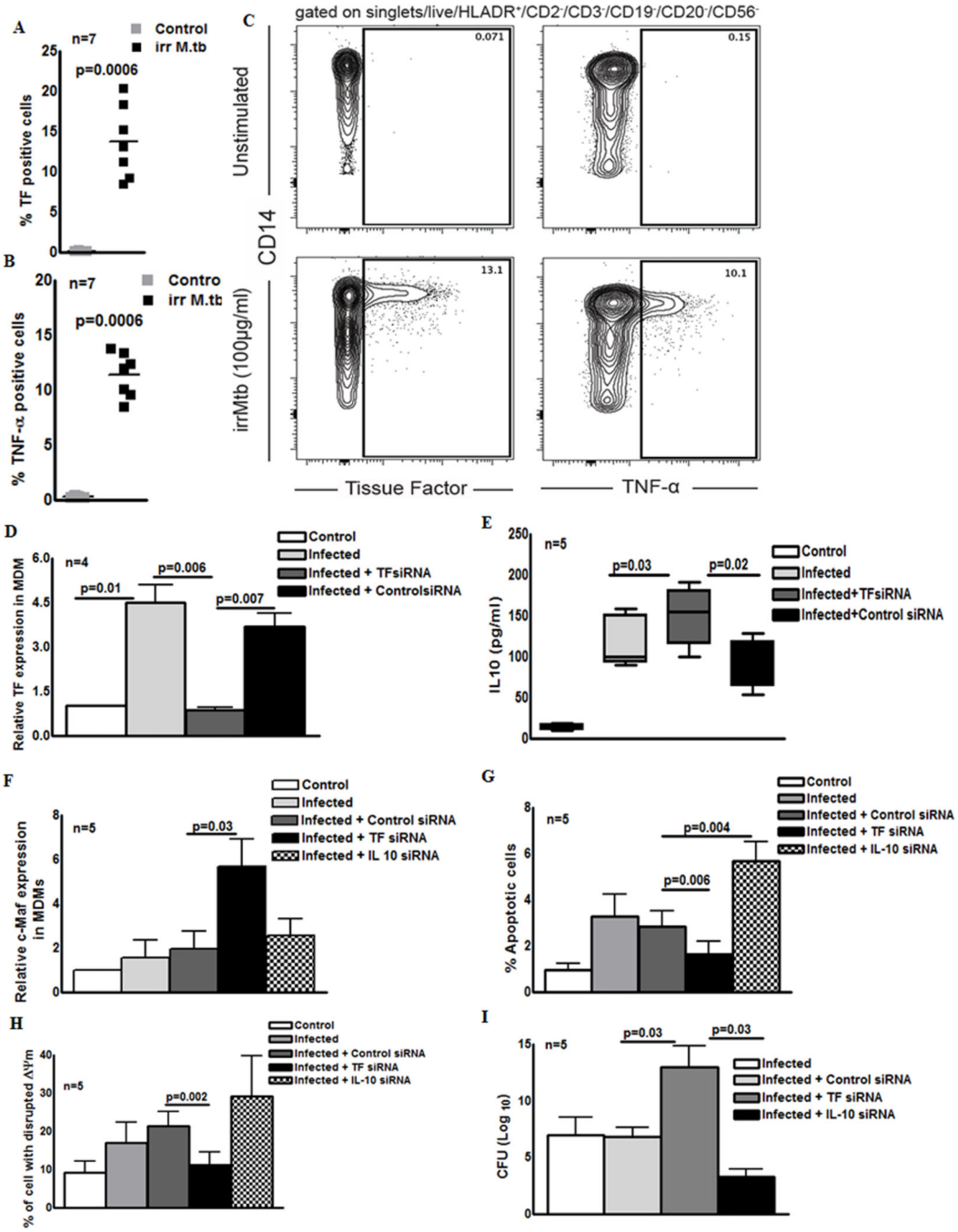

Fig. 7. TF regulates IL-10 production, apoptosis and *M. tb* growth in human MDMs

Expression of TF and TNF-α by CD14+ cells. PBMC from healthy donors were cultured with or without γ-irradiated *M. tb*. After 6 h CD14+ monocytes (HLADR+CD2-CD3-CD19-CD20-CD56-) were analyzed for the expression of **(A)** TF and **(B)** TNF-α using flow cytometry. **(C)** A representative flow cytometry plot is shown. All data are representative of the mean ± SEM of seven individual donors acquired in seven independent experiments were shown. Statistical analysis was performed using the one-way ANOVA followed by Bonferroni correction. MDMs from healthy donors were infected with H37Rv at a MOI of

1:2.5 (2.5 M. tb to one MDM). After 2 h, MDMs were washed to remove extracellular bacteria. Some cells were transfected with siRNA for TF or IL-10 (in some experiments) or scrambled siRNA. After 72 h, **(D)** TF expression was determined using real-time PCR. Gene expression was assessed by real-time PCR using the SYBR Green system and the ΔΔCT method for relative quantification. Fold changes in gene expression relative to uninfected MDMs are shown. All data are shown as the mean ± SEM of four individual donor sets and are representative of four independent experiments. Statistical analysis was performed using Student's *t*-test. **(E)** Culture supernatants were collected from five donor sets, and IL-10 levels were measured by ELISA. Data are shown as the median (horizontal line), and statistical analysis was performed using one-way ANOVA followed by Bonferroni correction. **(F)** c-Maf expression was determined using real-time PCR. Gene expression was assessed by real-time PCR using the SYBR Green system and the ΔΔCT method for relative quantification. Fold changes in gene expression relative to uninfected MDMs are shown. Statistical analysis was performed using the Student's *t*-test. **(G)** Apoptotic cells were determined using TUNEL assay. (H) Disrupted ΔΨm was determined by flow cytometry using a kit from Trevigen. All data are shown as the mean ± SEM and are representative of three independent experiments. Statistical analysis was performed using the Student's *t*-test. **(I)** After 7 days, CFU were measured. The results are shown as $\log_{10}$ CFU per well. All data are shown as mean ± SEM and are representative of the five independent experiments. Statistical analysis was performed using Student's *t*-test for bacterial counts.

Table I

List of primers used in the study

S.No	Gene name	Human Primer Sequences
1.	*GAPDH*	Forward: GCCATCAATGACCCCTTCATT Reverse: TTGACGGTGCCATGGAATTT
2.	Tissue Factor	Forward: CAGAGTTCACACCTTACCTGGAG Reverse: GTTGTTCCTTCTGACTAAAGTCCG
3.	IL-10	Forward: TCTCCGAGATGCCTTCAGCAGA Reverse: TCAGACAAGGCTTGGCAACCCA
4	c-MAF	Forward: TGCACTTCGACGACCGCTTCTCGG Reverse: AAGGTGGCTAGCTGGAATCGCG
S.No	**Gene name**	**Mouse Primer Sequences**
1.	β-actin	Forward: CCTTCAACACCCAGCCATGT Reverse: TGTGGACCACCAGAGGCATAC
2.	Tissue Factor	Forward: CATGGAGACGGAGACCAACT Reverse: CCATCTTGTTCAAACTGCTGA
3.	IFN-γ	Forward: TCAAGTGGCATAGATGTGGAAGAA Reverse: TGGCTCTGCAGGATTTTCATG
4.	IL-10	Forward: GGTTGCCAAGCCTTATCGGA Reverse: ACCTGCTCCACTGCCTTGCT
5.	IL-17	Forward: CTCCAGAAGGCCCTCAGACTAC Reverse: AGCTTTCCCTCCGCATTGACACAG
6.	c-MAF	Forward: AAATACGAGAAGTTGGTGAGCAA Reverse: CGGGAGAGGAAGGGTTGTC
7	CD-163	Forward: TCCACACGTCCAGAACAGTC Reverse: CCTTGGAAACAGAGACAGGC
8	iNOS	Forward: AACGGAGAACGTTGGATTTG Reverse: CAGCACAAGGGGTTTTCTTC
9	Arg1	Forward: TTGCGAGACGTAGACCCTGG Reverse: CAAAGCTCAGGTGAATCGGC
10	IL-12	Forward: GGAAGCACGGCAGCAGAATAA Reverse: CTTGAGGGAGAAGTAGGAATG
10	IL-1β	Forward: CAACCAACAAGTGATATTCTCCATG Reverse: GATCCACACTCTCCAGCT